ACS Catalysis

Review

pubs.acs.org/acscatalysis

Mechanistic Insights on Cooperative Catalysis through Computational Quantum Chemical Methods

Garima Jindal, Hemanta K. Kisan, and Raghavan B. Sunoj*

Department of Chemistry, Indian Institute of Technology Bombay, Powai, Mumbai 400076, India

ABSTRACT: One of the leading goals in contemporary chemical catalysis is to render improved efficiency to existing catalytic protocols. A few pertinent trends can readily be noticed from the current literature encompassing both catalysis development and applications. First, there has been an unprecedented growth in the use of metal-free organocatalytic methods toward realizing a plethora of synthetic targets. In parallel, the availability of newer and more efficient transition metal catalytic methods for the synthesis of complex molecules has become a reality over the years. The most recent developments indicate the emergence of multicatalytic approaches under one-pot reaction conditions, wherein the complementary attributes of two or more catalysts are made to work together. This domain, known as cooperative catalysis, is showing signs of immense promise. The mechanistic underpinnings of both of these forms of catalysis have been investigated by using a range of computational chemistry tools. With the availability of improved accuracy in computational methods aided by ever increasing computing technologies, the exploration of potential energy surfaces relating to complex cooperative catalytic systems has become more affordable. In this review, we have chosen a select set of examples from the emerging domain of cooperative catalysis to illustrate how computational methods have been effectively used toward gaining vital molecular insights. Emphasis is placed on mechanistic details, energetics of reaction, and, more importantly, on transition states that are responsible for stereoselectivity in asymmetric cooperative catalytic reactions.

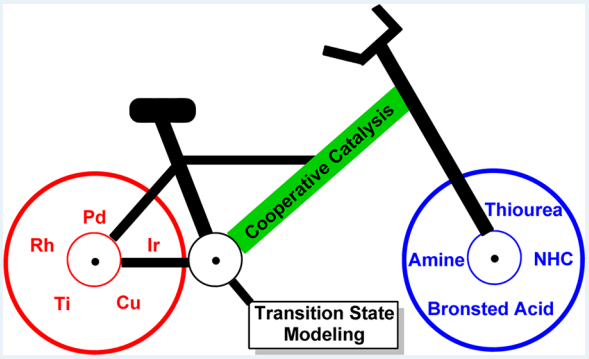

KEYWORDS: *organocatalysis, transition metal catalysis, cooperative catalysis, counterion, noncovalent interaction, stereoselectivity, density functional theory (DFT), transition state modeling*

INTRODUCTION

Design of newer and improved catalysts capable of asymmetric induction has remained in the forefront of research for several decades. In spite of the large number of organo[1] and transition metal catalyts[2] at their disposal, chemists remain in search for better catalytic protocols. While relatively smaller organic molecules act as catalyts, either by way of covalent or noncovalent activation of substrate(s) in organocatalysis,[1] transition metals nested into suitable ligands constitute the most common genre of organometallic catalysts.[2] Both of these forms of catalysis have been widely utilized in the domain of homogeneous catalysis. Interestingly, each of these catalytic approaches has its own advantages and disadvantages relative to the other.

A notably new and emerging trend in homogeneous catalysis relies on combining the advantages of both organo and transition metal catalysis under one-pot reaction conditions. The approach, which has come to be known as cooperative catalysis, appears to be a promising new strategy for asymmetric synthesis.[3] The most common version of cooperative catalysis typically employs a transition metal catalyst in conjunction with an organocatalyst.[4] Other modes including metal−metal[5] and organo−organo[6] have also been exploited. While the term cooperativity between two catalysts is used in a liberal sense in current literature, the question of whether the action of catalysts is in sequence or even noncooperative needs careful scrutiny.

There are some vital differences between other modes of catalysis, namely, bifunctional and sequential catalysis.[3c,7] A succinct representation of different modes in a multicatalytic scenario is provided in Figure 1. In a cooperative or synergistic system, the two catalysts (denoted as **Cat1** and **Cat2**) either are directly involved in the same catalytic cycle or are used in the activation of different substrates (**A** and **B**), which would eventually combine to give the final product (**P**). On the other hand, in sequential catalysis, the two catalysts activate substrates not in the same catalytic cycle but in a consecutive manner. In bifunctional catalysis, the same catalyst (**Cat1**) bears two catalytic sites, and these different sites are used to activate different substrates (**A** and **B**).[3c,7] In another dual catalytic situation, a double activation of the same substrate (**A**) by both catalysts (**Cat1** and **Cat2**) can take place. The two independent catalysts can either interact with each other via noncovalent interactions or only interact with

Received: October 30, 2014
Revised: December 5, 2014
Published: December 8, 2014

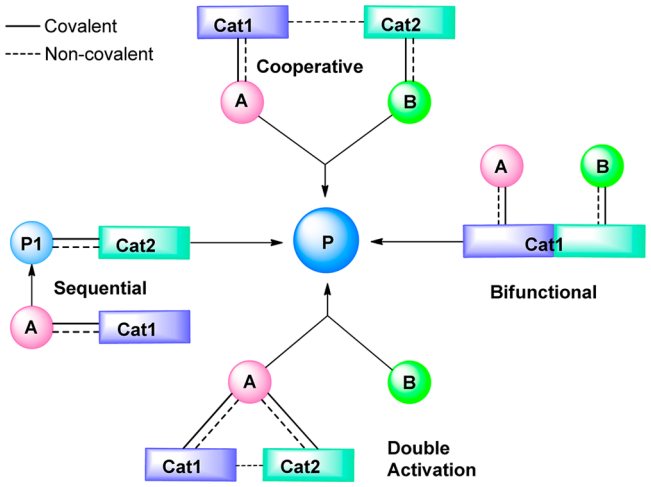

Figure 1. Various modes of catalysis involving multiple catalysts leading to product **P**.

the substrates. It should be noted that for an asymmetric reaction to be truly cooperative both catalysts should participate in the stereodetermining step. Thus, both catalysts along with the substrates should form an organized transition state, which will help to transfer the chiral information to the product and eventually lead to stereoselectivity.

The use of both transition metal and organocatalyst opens up a whole new area in asymmetric synthesis. In the realm of emerging cooperative catalysis, the inspiration derived from enzymatic catalysis should be acknowledged for its use in biological and chemical systems to carry out reactions with high efficiency and selectivity. In biological systems, acids and bases have been known to activate the substrates within an active site. For instance, acetylcholinesterase is hydrolyzed to acetate and choline in a concerted manner by a catalytic triad consisting of three amino acid residues such as a serine, histidine, and glutamate.[8] Enzymatic reactions offer an elegant demonstration of how cooperative action, wherein different noncovalent and electrostatic interactions take place within the active site, can stabilize a transition state.[9]

The cooperativity by different catalysts in a given reaction can be achieved through a suitable mode of activation of the substrates. Substrate activation via the formation of covalent bonds or via weak noncovalent interactions is the most widely proposed methods. In the noncovalent mode, the reacting substrates are typically held together by different regions of a multicatalytic system, such as in the case of a bifunctional catalyst.[9a,10] One or a combination of interactions, such as H-bonding, ionic, $\pi-\pi$, cation$-\pi$, is generally thought to play a critical role in such asymmetric multicatalytic reactions.

IMPORTANCE OF TRANSITION STATE MODELING IN COOPERATIVE CATALYSIS

While there have been different cooperative catalytic combinations reported in the literature, the design of newer variants would certainly be benefited by mechanistic studies. A major challenge in devising new catalytic systems is the compatibility between the catalysts. More importantly, the mode in which cooperativity is achieved is not well understood for many reactions that have been proposed to rely on this concept. An improved understanding of the role of individual catalysts and how they act in tandem is of prime significance. Similarly, whether the two catalysts cooperatively function throughout a catalytic cycle is also of importance. It is quite possible that multiple catalysts are required only in a few steps of the reaction. In the other steps of the reaction, a single catalyst can perform the desired task. Another possibility is a sequential mode of catalysis, wherein at no point in time do the two catalysts act together. They activate different substrates in a sequential manner. Such molecular level details are of importance to provide additional impetus to the development of cooperative multicatalytic approaches. As with the developments in other catalytic reactions involving single catalysts, computational studies are known to be capable of providing valuable molecular insights. The above-mentioned details can certainly be sought through rigorous computational analysis of cooperative catalytic systems.

The advantages of the insights gained through computational studies are 2-fold. First, it can help to rationalize the mechanism and the origin of stereoselectivity. Second, these insights can contribute to the rational design of asymmetric catalysis. Computationally aided catalyst design would further promote synergism between the use of modern theoretical methods and practical synthesis. Knowledge of the stereoelectronic factors operating in the key transition states of the reaction, energies of the intermediates, nature of the active catalysts, and the potential resting state can all provide valuable inputs in the design of newer catalyst combinations for multicatalytic applications. A deeper understanding of the functioning of two catalysts in concert will be useful in achieving improved control over the stereoselectivity in cooperative catalysis.

The present review provides an overview of the mechanistic studies on cooperative catalysis that employ quantum chemical methods. Herein, we aim to emphasize and provide clarity on a subset of some carefully chosen examples rather than attempting to undertake an exhaustive treatise of cooperative catalysis. While the focus of our discussions is in the area of asymmetric cooperative catalysis, a few important examples of achiral catalysts are also included. This review is organized in two major sections: the first half encompasses the domain of cooperative catalysis involving organocatalysts and transition metal catalysts, and the second section is devoted to the combination of two organocatalysts. On the basis of the type of organocatalysts involved, the first section is further grouped into subsets of examples.

COMPUTATIONAL STUDIES ON ORGANO AND TRANSITION METAL CATALYSIS

Over the years, computational chemistry methods have witnessed a steady growth, both in terms of being able to handle more realistic molecules as well as in its accuracy.[11] Ever-increasing computing technology has enabled incorporation of the effect of medium and other external perturbations in the usual scheme of things.[12] Increased reliability of ab initio and density functional computations has helped in gaining valuable insights into the structure, property, and reactivities of molecules and materials. To say the least, improved clarity on various reaction mechanisms has been effectively accomplished by using first-principles computational methods.[11] In a typical mechanistic investigation, density functional theory (DFT) is generally employed in conjunction with a suitable basis set. The choice of functional for many organometallic and organocatalytic reactions has remained the B3LYP until recently. It has been known to

dx.doi.org/10.1021/cs501688y | ACS Catal. 2015, 5, 480−503

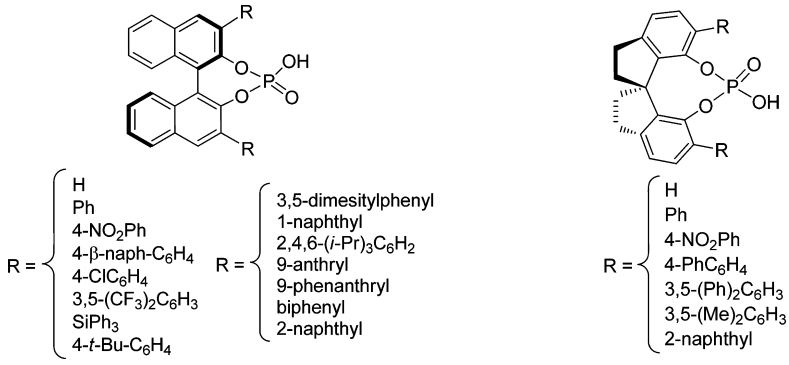

Figure 2. Examples of commonly found axially chiral Brønsted acids used in multicatalytic reactions in conjunction with transition metals.

perform quite well for stereoselective reactions. However, in the domain of cooperative catalysis, wherein the molecular systems are of increasingly larger size, dispersion effects are expected to play a key role. Hence, other modern DFT functionals such as the meta-GGA functionals, double hybrid functionals, and functionals that can treat long-range dispersion are being employed in the study of such complex systems.

COMPUTATIONAL STUDIES ON COOPERATIVITY BETWEEN METAL AND ORGANO CATALYSTS

Among the plethora of successful organocatalysts, the ones found to have good compatibility for being employed in conjunction with transition metals are amines,[1d,13] cinchona,[14] N-heterocyclic carbenes (NHCs),[15] and Brønsted acids.[16] Akin to the organocatalysts, there have been several transition metal catalysts (e.g., Pd, Au, Rh, Ru, Ir) that have found successful applications in asymmetric catalysis. The combinations that can be created by using these transition metals and organocatalysts are quite overwhelming. Such multicatalytic approaches can offer impressive methodologies for the synthesis of complex target molecules with increasingly precise control over the stereochemical outcome. There have been computational efforts toward establishing the reaction mechanism of cooperative catalysis involving transition metals and organocatalysts of the above kind. The following section provides a succinct view of the current mechanistic understanding.

Transition Metal−Brønsted Acid Cooperative Catalysis. The use of chiral Brønsted acids in conjunction with different transition metals is one of the most widely employed cooperative catalytic strategies today. Chiral Brønsted acids have been proven to be successful as organocatalysts in a host of different reactions.[16] The use of chiral Brønsted acids was initiated by Terada and Akiyama in 2004.[17] These most commonly used Brønsted acids, belonging to the phosphoric acid family, are proposed to promote organocatalytic reactions via the formation of ion pairs.[18] The chiral phosphoric acids can be derived either from a binol or from a spirocyclic framework known as spinols, as shown in Figure 2. An ample number of mechanistic studies, including suitable transition state models, on chiral Brønsted acid-catalyzed stereoselective reactions has been reported. The stereocontrol is suggested to emanate from the bulkier substituents typically present at the 3,3′ positions of the binol framework.[19]

One of the most common strategies in asymmetric transition metal catalysis involves the use of a chiral ligand directly bound to the metal.[2] While this approach has been successful toward inducing good stereoselectivity in a plethora of reactions, certain issues associated with controlling reactivity and selectivity still persist. Control over the reactivity−selectivity issue in such forms of asymmetric catalysis is related to the requirement that the substrate and chiral entity are typically bound to each other, such as in a single-site catalysis scenario. One can envisage an alternative approach wherein the catalyst does not interact with the rest of the reacting system via a strong bond; instead, it should be allowed to develop only a series of weak interactions.[9a,20] This would enable the use of one type of chiral catalyst across a broader range of reactions without having to synthesize transition metal catalysts with varying chiral ligand combinations.

A most recently developed concept relies on the ion pair mode of catalysis.[21] The idea behind using chiral anions came into being perhaps due to omnipresent cationic intermediates in several transition metal catalyzed reactions. A successful chiral counterion could ideally be used for a range of related reactions. On the basis of this premise, chiral counterions derived from binol phosphoric acids have, in fact, been successfully used in a variety of transition metal-catalyzed reactions.[22] The term asymmetric counteranion directed catalysis (ACDC) was coined to encompass a series of reactions that are believed to proceed via ion pairs.[23] Despite the popularity of such multicatalytic reactions, transition state models for cooperative catalytic systems comprising metals and Brønsted acids continue to remain scarce. The mechanistic ambiguities associated with the simultaneous use of Brønsted acids and transition metals relate to the extent of cooperation between the two catalysts and the lack of clarity surrounding the exact role of the Brønsted acid. Even though several previous reports have echoed these issues, there are only a few that have attempted to explicitly address it. The use of chiral phosphoric acids or the direct use of chiral phosphates opens up different mechanistic scenarios.[24] The overlap between the varying modes of catalysis governed by H-bonding, anionic ligand, or counterion is not quite evident and is still a matter of considerable controversy.

Rueping and co-workers first reported the use of chiral Brønsted acids in conjunction with transition metals back in 2007.[25] Toste and co-workers reported Au−phosphoric acid-catalyzed hydroamination, hydroalkoxylation, and hydro-

dx.doi.org/10.1021/cs501688y | ACS Catal. 2015, 5, 480−503

Scheme 1. Ir−Brønsted Acid-Catalyzed Carbocyclization of 1,6-Enynes

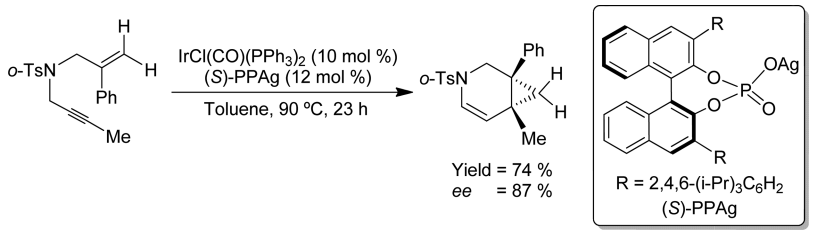

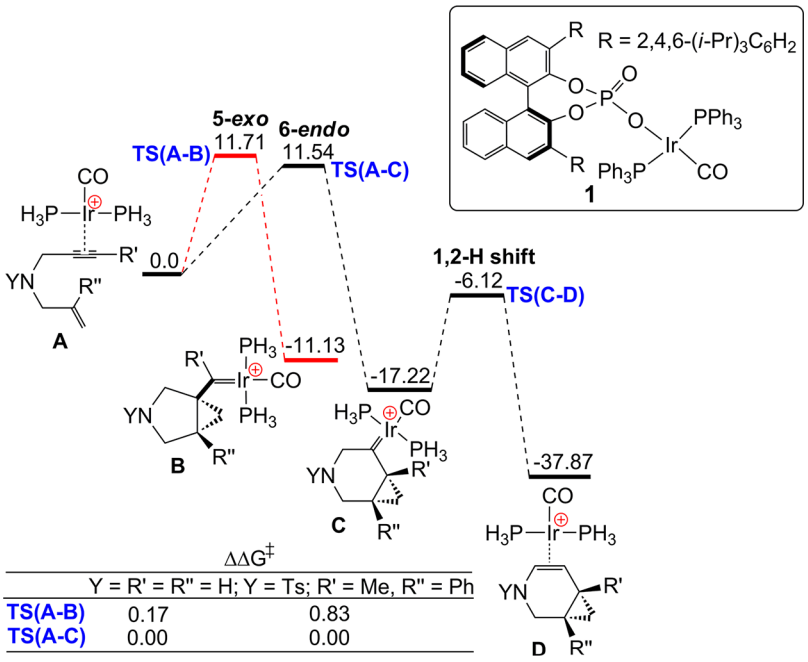

Figure 3. Free energy profile (kcal/mol) at the B3LYP/6-31G(d,p),LANL2DZ(Ir) level of theory for the cyclization of enynes mediated by $[Ir(CO)(PH_3)_2]^+$. Values given in the free energy profile correspond to Y = R′ = R″ = H.

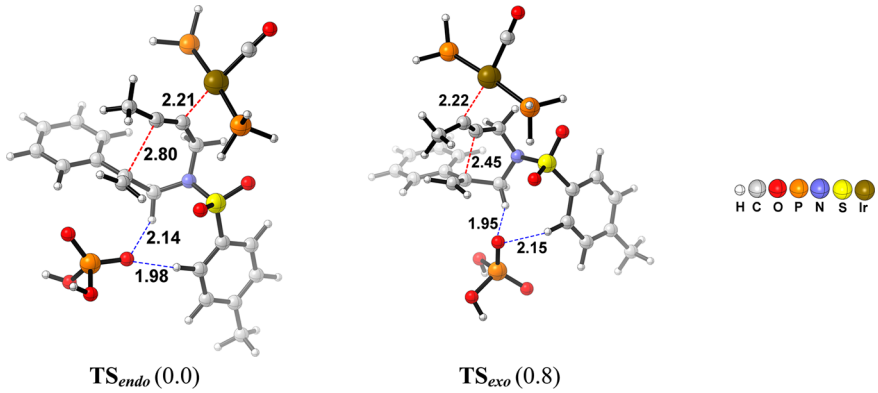

Figure 4. Optimized 6-*endo* and 5-*exo* transition states for the carbocyclization of enynes. Relative free energies (kcal/mol) at the B3LYP/6-31G(d,p),LANL2DZ(Ir) level of theory are given in parentheses. All distances are in angstroms.

carboxylation of allenes.[26] Chiral ligands such as phosphines, even though successful for several other reactions, failed to yield selectivities >10% in this case. In contrast, the use of achiral Au complexes and chiral silver phosphates yielded excellent stereoselectivities. Since then, various transition metals such as Au, Rh, Ru, Pd, Ag, Ir, Cu, and so on have been demonstrated to be effective when employed together with these chiral acids.[4e,27] Parallel efforts by other leading groups have offered interesting examples of chiral counterions as a source for chiral induction.

There have been a few computational studies using density functional theory methods on model systems that aimed to rationalize the role of the counterions. Barbazanges et al. performed a combined experimental and computational study to shed light on the nature of active species and the role of counterion.[28] An iridium catalyst was used to synthesize chiral bicyclo[4.1.0]hept-2-enes in good stereoselectivities (up to 93%) from 1,6-enynes (Scheme 1). The chirality has been induced by using a chiral silver phosphate. ^{31}P NMR spectroscopy was used to gain insight into the structure of

dx.doi.org/10.1021/cs501688y | ACS Catal. 2015, 5, 480−503

the active species. The exchange of the chloride ligand on iridium with the chiral phosphate has been suggested to be responsible for the formation of complex **1**, as shown in Figure 3. Subsequently, DFT calculations (B3LYP/6-31G-(d,p),LANL2DZ(Ir)) were carried out to study the mechanistic details. The model systems used for the calculations are shown in Figure 3. Instead of PPh_3, PH_3 was chosen, the N-tosyl group was replaced with a simple N−H, and no substituents were used on the enyne.

The 6-*endo-dig* cyclization was noted to be marginally more preferred over 5-*exo-dig* cyclization. Further optimization was carried out in the presence of a model phosphate, HPO_4^- (Figure 4). Again, the *endo* pathway was identified as being more favored over the *exo* pathway. Attempts to locate the phosphate counterion in the vicinity of the metal center led to its repulsion from the coordination sphere. Increasing the coordination number around Ir also led to the repulsion of either of the ligands (CO and PH_3). Subsequently, the phosphate ion was positioned in a manner that allows the formation of weak hydrogen bonds to the C−H groups of the substrate. These weak interactions are suggested to hold the key to the observed stereoselectivity.

Additional studies are desirable with the actual ligands and catalysts to fully establish the mechanism and origin of stereoselectivity of the reaction shown in Scheme 1. The role of chiral counterion in inducing the stereoselectivity would become clear only through such a complete study. Interestingly, the detection of complex **1** (Figure 3), in which the phosphate is coordinated to the metal, hints at a potential participation of the chiral phosphate as a ligand rather than a counterion. The replacement of a PPh_3/CO ligand with a phosphate while maintaining a tetracoordination around Ir will be an interesting alternative to examine.

Another report by Gandon, Roulland, and co-workers involves the Pd-catalyzed synthesis of substituted tetrahydrofurans, as shown in Scheme 2.[29] Even though an external source of acid was not introduced into this system, the counterion generated by the ionization of the substrate can participate in the mechanism. Interestingly, the counterion was found to have a direct effect on the observed diastereoselectivity.

Scheme 2. (i) Synthesis of Substituted Tetrahydofurans Using a Tsuji−Trost Reaction and (ii) Correlation between the pK_a Value of the Conjugate Acid of the Counterion and Diastereomeric Ratio of the Cyclic Products[a]

(i)

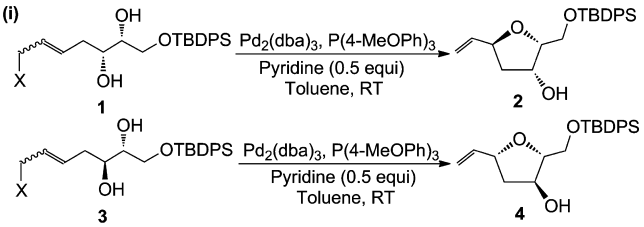

(ii)

Entry	Leaving group or counterion (X^-)	Relative configuration of **1** and **3**	d.r.	p*Ka* of HX in H_2O
1	$MeCO_2^-$	*syn* (**1**) *anti* (**3**)	92:8 (**2/2'**) 94:6 (**4/4'**)	4.76
2	*tert*-$BuCO_2^-$	*syn* (**1a**) *anti* (**3a**)	96:4 (**2/2'**) 95:5 (**4/4'**)	5.01
3	*p*-$MeOPhCO_2^-$	*syn* (**1b**) *anti* (**3b**)	90:10 (**2/2'**) 90:10 (**4/4'**)	4.47
4	$PhCO_2^-$	*syn* (**1c**) *anti* (**3c**)	88:12 (**2/2'**) 86:14 (**4/4'**)	4.20

[a]The cation involved is a Pd-π-allyl species generated from the substrate upon departure of the leaving group X.

The crucial requirement of the acetate ion and its role in controlling the selectivity were established by using DFT-(B3LYP) computations. In addition to the obvious H-bonding interactions with the cyclizing hydroxyl group of the substrate, the acetate also engages in H-bonding to the β-OH group of the substrate in both of the selectivity-determining transition states (Figure 5). The lower energy diastereomeric transition state, **TS(*allyl-R*-2)**, exhibits two additional stabilizing interactions. A vital H-bonding (C−H···O (2.10 Å)) between the counterion acetate and the allyl substrate is noted along with a Pd···O interaction. Interesting corroboration of these computational insights was borne out by additional experiments wherein poorer yields and slower rates were noticed when substrates with a protected β-OH group were used. The importance of the C−H···O interaction in controlling the selectivity was further proven by isotopic labeling studies. Deuteriation of the C−H group of the substrate (hydrogen atom inscribed in a red circle, as shown in Figure 5) resulted in a decrease in the diastereoselectivity from 96:4 to 91:9. This was attributed to the weaker C−D···O interaction as compared to the C−H···O bond. While the report offers important and timely details of counterions in stereoselectivity, transition states in the absence of the counterion as well as an additional mode wherein the acetate is directly coordinated to Pd could have provided a more comprehensive understanding of the role of counterions.

In another interesting study, Iggo, Xiao, and co-workers probed cooperativity between an Ir catalyst and chiral phosphoric acid by using both experimental and computational methods (Scheme 3).[30] They employed a combination of NMR spectroscopy, diffusion measurements, and NOE-constrained computations. The NOE signals were used to identify the nature of interactions among different species involved in the reaction. On the basis of these interactions, constraints were set up for computational modeling. These insights were employed toward offering mechanistic clarity on the hydrogenation of imines.

The authors addressed a few very pertinent questions, such as (a) the role of chiral phosphoric acid in inducing enantioselectivity, (b) the origin of stereocontrol, and (c) the nature of the actual species involved in the stereoinducing step. It was first established whether the stereoselectivity arises in the hydride transfer or in the enantioselective formation of complex **C** (Scheme 3ii). NMR analyses revealed that complex **C** formed during catalysis is a racemic mixture that could be further isolated. The possible diastereomers of complex **C** are given in Scheme 3. Reduction of the iminium−phosphate complex $[\mathbf{1H}]^+[\mathbf{A}]^-$ in the presence of a racemic mixture of **C** led to similar enantioselectivity as that obtained through the catalyzed process. Thus, the enantioselective generation of **C** is not to be regarded the stereoinducing step. The reaction of **C** with imine **1** failed to yield any product, indicating that the iminium cation is absolutely necessary for the success of this reaction. To gain further insights into the nature of bonding in complex **C**, the iminium cation ($\mathbf{1H}^+$), and the chiral phosphate anion ($\mathbf{A}^-$), NMR studies were carried out. It was concluded that the three species are held together primarily by H-bonding interaction. NOE, DFT(B3LYP), and semiempirical PM6

dx.doi.org/10.1021/cs501688y | ACS Catal. 2015, 5, 480−503

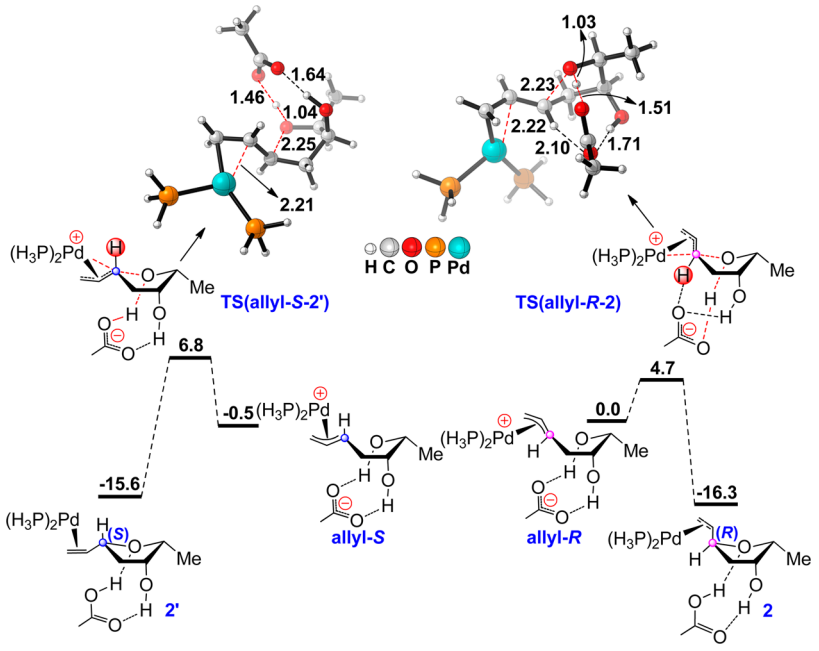

Figure 5. Free energy profile (kcal/mol) and the stereodetermining transition states for the formation of major (**2**) and minor (**2′**) substituted tetrahydrofurans in a Tsuji−Trost reaction obtained at the B3LYP/6-31+G(d,p),SDD(Pd) level of theory. All distances are in angstroms.

Scheme 3. (i) Hydrogenation of Imines by an Iridium Catalyst (B) and a Chiral Phosphoric Acid (HA) and (ii) Mechanism of Formation of an Amine Product (2)

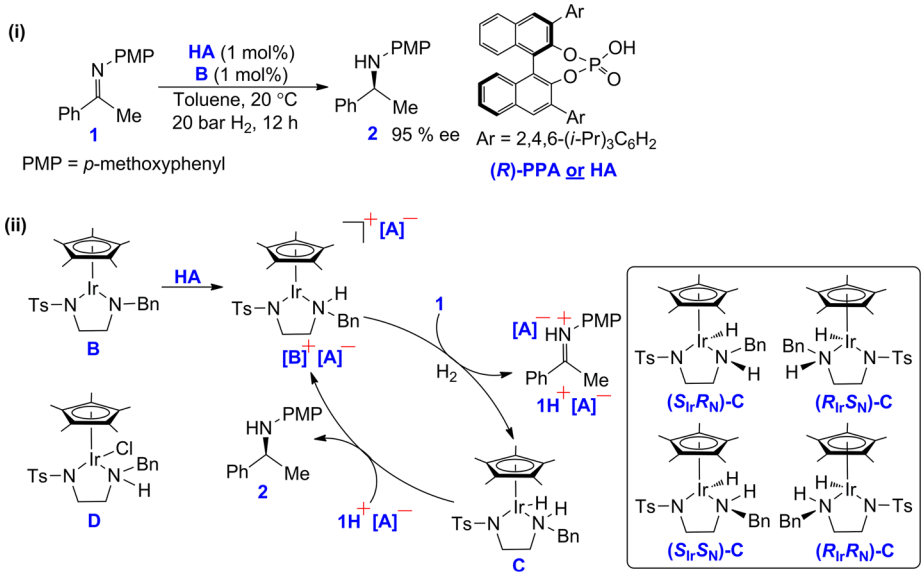

calculations were used to probe the nature of the ternary complexes (Figure 6) formed among iridium complex **D**, phosphate anion $\mathbf{A}^-$, and iminium cation $\mathbf{1H}^+$. It was found that the ternary complex arising from the *cis* isomer of **D** has multiple C−H···π interactions, which are absent in the corresponding *trans* isomer. These weak interactions led to a lower energy of the *cis* analogue by about 3 kcal/mol. The three species, **D**, $\mathbf{A}^-$, and $\mathbf{1H}^+$, are held together via noncovalent interactions, which are suggested to be critical to the observed stereoselectivity. It would be interesting to examine the transition states for the hydrogenation step and the factors that govern the stereoselectivity. More importantly, it would require additional analysis to verify whether the factors governing the stability in the ternary complexes could have a direct bearing on the transition state geometries as well.

In keeping with the contemporary trends in asymmetric catalysis on the use of multiple catalysts under one-pot reaction conditions, List and co-workers reported an exquisite catalytic triad consisting of a transition metal (Pd), chiral phosphoric acid, and a secondary amine toward generating a quaternary chiral center through an asymmetric allylation reaction.[31] This represents a unique example of a cooperative multicatalytic system wherein the mode of action is far more complex owing to numerous possible combinations (Scheme 4).

In a very recent study, Jindal and Sunoj reported a comprehensive DFT (M06 and B3LYP) investigation on the

dx.doi.org/10.1021/cs501688y | ACS Catal. 2015, 5, 480−503

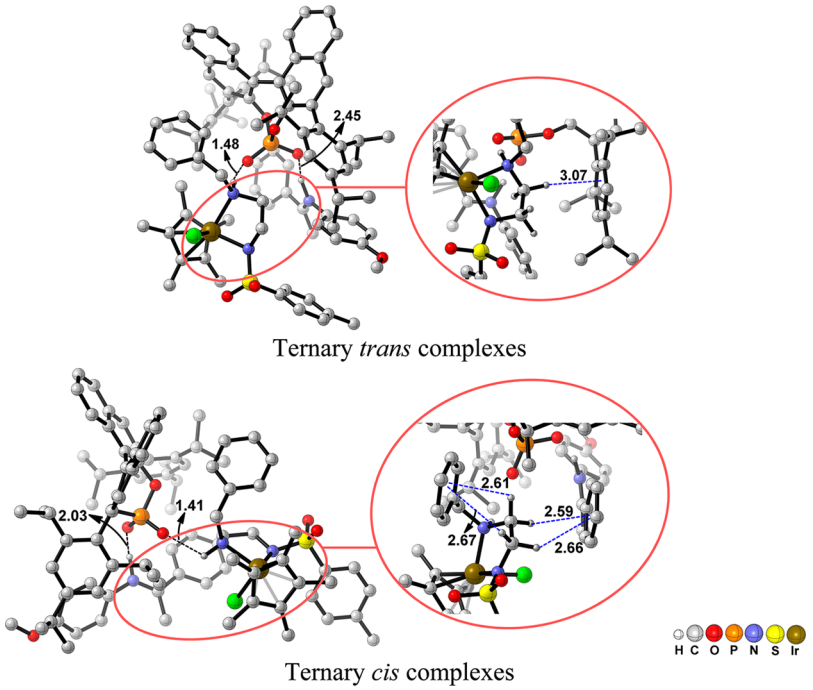

Figure 6. Optimized geometries of ternary complexes for *trans* and *cis* isomers with the iridium complex **D**, phosphate anion $\mathbf{A}^-$, and iminium cation $\mathbf{1H}^+$ exhibiting H-bonding and C−H···π interactions, as obtained at the B3LYP/6-31G(d,p),LANL2DZ(Ir) level of theory. All distances are in angstroms.

Scheme 4. Pd−Brønsted Acid Catalyzed Allylation of Aldehydes[a]

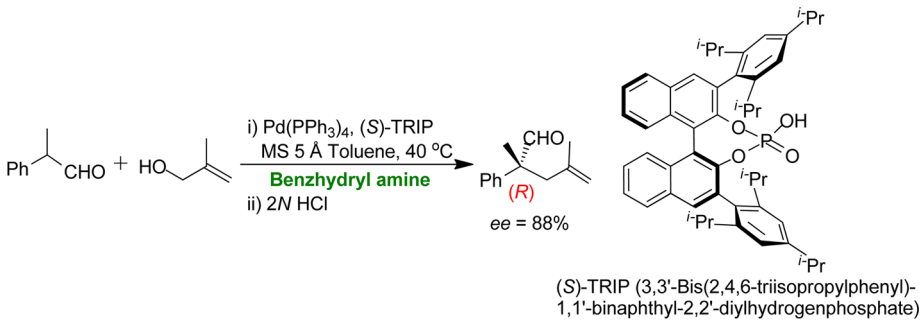

[a]Reprinted from ref 32. Copyright 2014 American Chemical Society.

mechanism of this reaction to shed light on the nature of cooperativity and the role of chiral phosphoric acid.[32] The reaction was suggested to involve the formation of an enamine **a** (formed between the aldehyde and the amine), which could make use of acid catalysis offered by the phosphoric acid (Scheme 5). In this case also, the selectivity was suggested to be governed by ion pair formation between the chiral phosphate and Pd-π-allyl species **b** (generated by the action of phosphoric acid on allylic alcohol) with which the incoming enamine reacts. Thus, the chiral phosphoric acid can play multiple roles, in addition to influencing the stereoselectivity. The authors have addressed an important question on the mode of catalysis so as to establish whether the phosphate counterion transfers chirality through selective H-bonding interactions with the N−H group of the enamine[19,33] or through ion pair formation.[23,27,31]

Since the initial source of palladium is bulky $Pd(PPh_3)_4$, its dissociation into smaller analogues and combination with the substrate are quite desirable. The authors first examined the role of different likely active species, such as **1a**, **1b** and **2**, that differ in the number of phosphine ligands on Pd (Scheme 5ii). It is worth noting that in the previous examples described in this review the chiral phosphate ion was considered to be only a counterion typically positioned in the outer-sphere but not a ligand bound to the transition metal. The computed relative energies indicated that a *bis*-(triphenylphosphine)−Pd-π-allyl complex **2** was more preferred over other active species. The difference in energies of the active species when the phosphate is bound directly to Pd (**1a**) and when it remains in the outer sphere (**2**) was noted to be only 0.8 kcal/mol in the condensed phase, suggesting that the nature of the active species could be different in different reactions.

In the stereoselective C−C bond formation transition states, the authors examined the likely involvement of both **1a** and **2** as the potential active species. The energy of transition states with **1a** was reported to be of higher energy (13 kcal/mol). On the basis of the relative energies, *bis*-(triphenylphosphine)−Pd-π-allyl (**2**) was suggested to be the most important active species participating in the enantioselectivity controlling step of the reaction. The vital point to note is that

dx.doi.org/10.1021/cs501688y | *ACS Catal.* 2015, 5, 480−503

Scheme 5. (i) Transition State Model for the Stereocontrolling C−C Bond Formation between Pd-π-allyl and Enamine Derived from Benzylaldehyde and (ii) Potential Active Species and Relative Free Energies (kcal/mol) in the Gas Phase (Normal Font) and in the Condensed Phase at the $SMD_{toluene}$/M06/6-31G(d,p),LANL2DZ(Pd)//M06/6-31G(d,p),LANL2DZ(Pd) Level of Theory (Italics)[a]

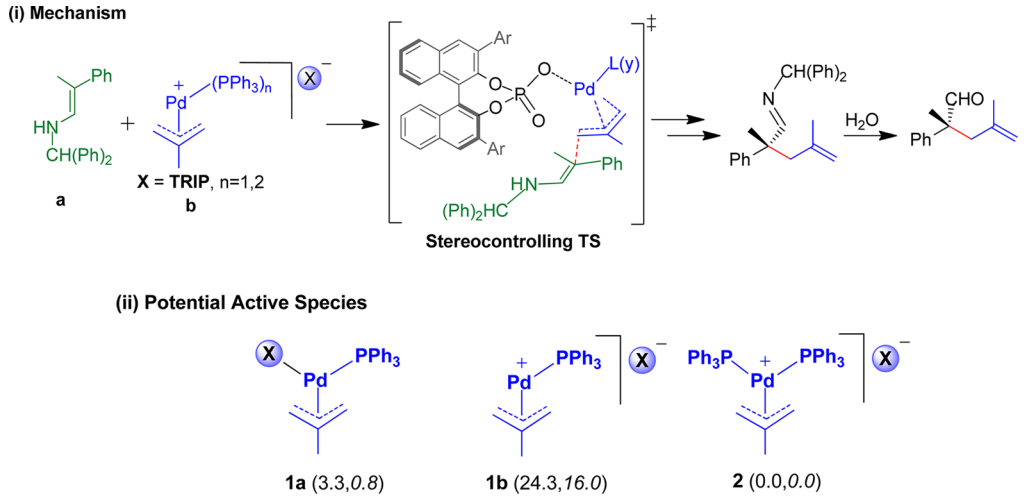

[a]Reprinted with from ref 32. Copyright (2014) American Chemical Society.

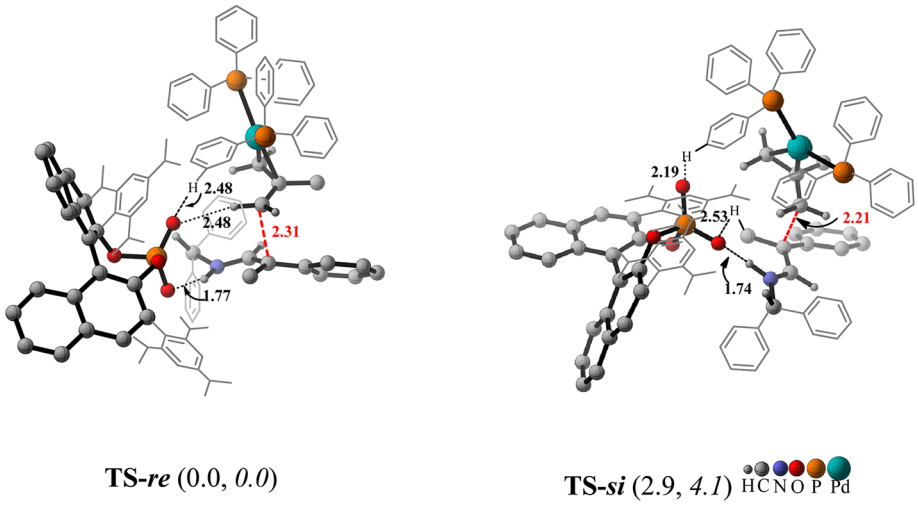

Figure 7. Optimized geometries of the lower energy transition states for stereocontrolling C−C bond formation involving a TRIP catalyst in the case of active species **2**. The relative free energies (kcal/mol) at the M06/6-31G(d,p),LANL2DZ(Pd) and $SMD_{toluene}$/M06/6-31G(d,p),LANL2DZ(Pd)//M06/6-31G(d,p),LANL2DZ(Pd) levels of theory are provided in parentheses using normal and italics fonts, respectively. All distances are in angstroms. Reprinted from ref 32. Copyright 2014 American Chemical Society.

Scheme 6. Palladium and Brønsted Acid Cooperative Catalytic Method for the Formation of Spirocyclic Indenes[a]

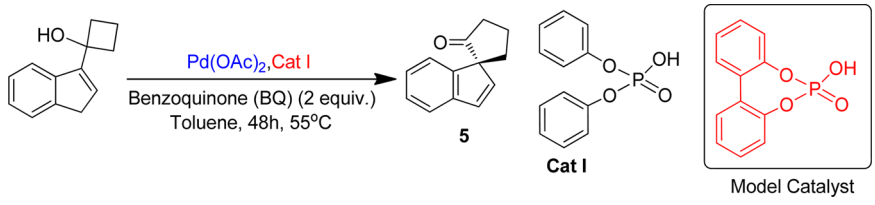

[a]A model phosphoric acid, shown in the inset, was used in the mechanistic investigation.

in active species **2** the chiral counterion remains in the outer-sphere, instead of directly binding to the metal, as is generally proposed in transition metal catalysis. The energy difference between the diastereomeric transition states **TS-*re*** and **TS-*si*** was found to be 2.9 kcal/mol, which corresponds to an *ee* of 99% in favor of the *R* enantiomer and is in excellent agreement with the experimental value of 88%.

The transition state models were also employed to shed light on the origin of chiral induction. A number of weak interactions that differ between the diastereomeric transition states were highlighted. First, the Pd···$O_{phosphate}$ distances in

dx.doi.org/10.1021/cs501688y | ACS Catal. 2015, 5, 480−503

Scheme 7. Two Different Pathways for the Formation of Spirocyclic Product (5)

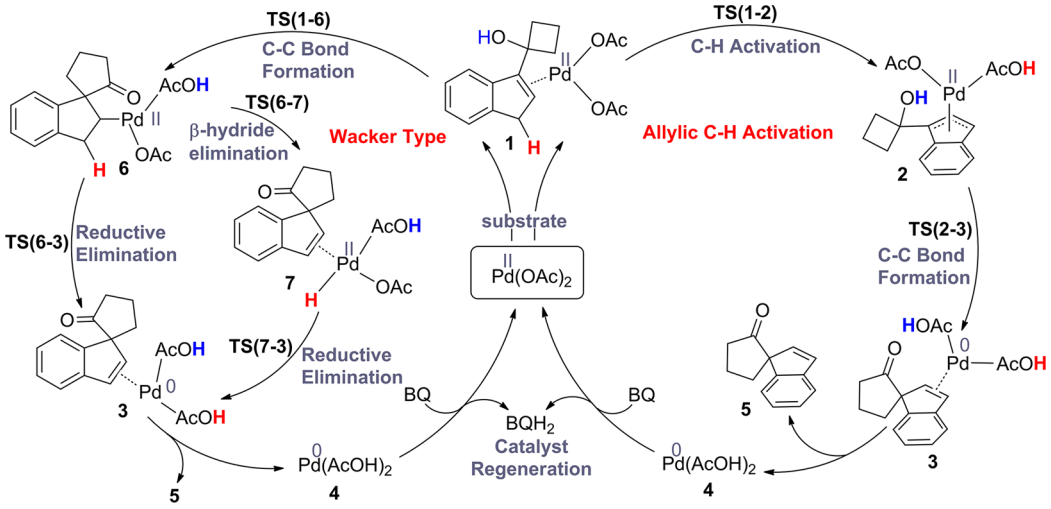

both the stereocontrolling transition states were more than 4.5 Å, ruling out any direct interaction between Pd and the phosphate counterion (Figure 7). The chiral phosphate counterion was shown to exhibit other interactions such as an ionic hydrogen bond[34] between the enamine N−H and the phosphate oxygen (1.77 Å in **TS-*re*** and 1.74 Å in **TS-*si***) and C−H···O interactions[35] between the *bis*-(triphenylphosphine)−Pd-π-allyl moiety and the phosphate oxygen. The noncovalent interactions between the substrates and the chiral counterion result in a suitable stereochemical disposition between the prochiral faces of the reacting partners conducive for stereoselective C−C bond formation. The study, therefore, offered a convincing picture on the role of counterion controlled chiral induction.

In another recent study, Jindal and Sunoj reported the mechanism of a dual catalytic Pd(II)−Brønsted acid-catalyzed formation of spirocyclic indenes, as shown in Scheme 6.[36] This cooperative catalytic reaction provides access to a spirocyclic skeleton bearing a quaternary carbon center, which is found in several biologically relevant molecules.[37] The synthesis of such compounds is known to be a difficult task.[38] It is interesting to note that, in a one-pot reaction, palladium acetate catalyst, Brønsted acid (**Cat 1**), oxidant BQ, and water are all present together in the reaction mixture, opening up myriad mechanistic possibilities.

Two most likely mechanistic possibilities, as shown in Scheme 7, were examined. These differ in the timing of ring-expansion step. The first one involves an allylic C−H activation, whereas the other route is through a Wacker-type process. In the allylic pathway, allylic C−H bond activation was proposed to take place in the initial catalyst−substrate complex (**1**), via **TS(1−2)**, to give Pd-π-allyl intermediate **2**. A semipinacol type rearrangement in **2** results in ring expansion of the cyclobutanol to spirocyclic intermediate **3**. The C−C bond formation transition state **TS(2−3)** was shown to be accompanied by a concomitant reductive elimination, wherein the proton from the cyclobutanol OH group is transferred to the Pd-bound acetate. On the other hand, the Wacker-type pathway involves a semipinacol ring expansion in **1** first via **TS(1−6)** to provide a spirocyclic intermediate (**6**). This intermediate can undergo (i) an acetate-assisted deprotonation (via **TS(6−3)**) to directly yield the product complex (**3**) or (ii) a β-hydride elimination to give a Pd−hydride intermediate (**7**), which would be followed by a reductive elimination to give the product. The catalytic cycle can be sustained by the action of benzoquinone, which would oxidize Pd(0) to Pd(II).[39] The authors attempted to understand the cooperative action of Pd and the Brønsted acid in addition to exploring the likely role of other additives such as BQ and H_2O. This goal has been accomplished by considering different active species using a model catalytic system, as shown in the inset in Scheme 6, in different steps of the reaction.

A fairly large number of combinations of ligands on palladium were examined in an effort to identify the most likely active species involved in the reaction. Interestingly, this dynamic ligand exchange was considered for all significant steps of the catalytic cycle. A summary of computed Gibbs free energies obtained by using DFT(M06) method for several ligand combinations for important transition states is provided in Figure 8. On the basis of these data, the authors emphasized the significance of ligand exchanges in each step of the reaction. For instance, the Gibbs free energies provided in Table 1 show that the replacement of acetate by phosphate, in general, offers additional stabilization to the transition states. The *bis*-phosphate ligands on palladium were noted to be consistently more preferred over the native *bis*-acetate in both the allylic and Wacker pathways. In the case of the allylic C−H activation pathway, BQ was identified as being a more preferred ligand on palladium in the ring-expansion transition state (Figure 8). Even more interesting, BQ was noted to be a less preferred ligand in the Wacker-type process, both in C−C bond formation and the subsequent reductive elimination steps. Another important feature of their mechanistic investigation relates to the finding that the lower energy pathway was a Wacker-type process rather than an allylic C−H activation pathway. The overall study indicated the importance of simultaneous participation by both Pd and the Brønsted acid in the reaction.

Another important class of transition metal catalysts that has been widely used in conjunction with other catalysts under multicatalytic conditions is dirhodium carboxylates.[40] The catalytic ability of this family has been exploited by making use of donor−acceptor carbenoids derived from dirhodium carboxylates.[41] Insertion of dirhodium carbenoids to C−X bonds (where X = N, O, S) has offered interestingly

dx.doi.org/10.1021/cs501688y | ACS Catal. 2015, 5, 480−503

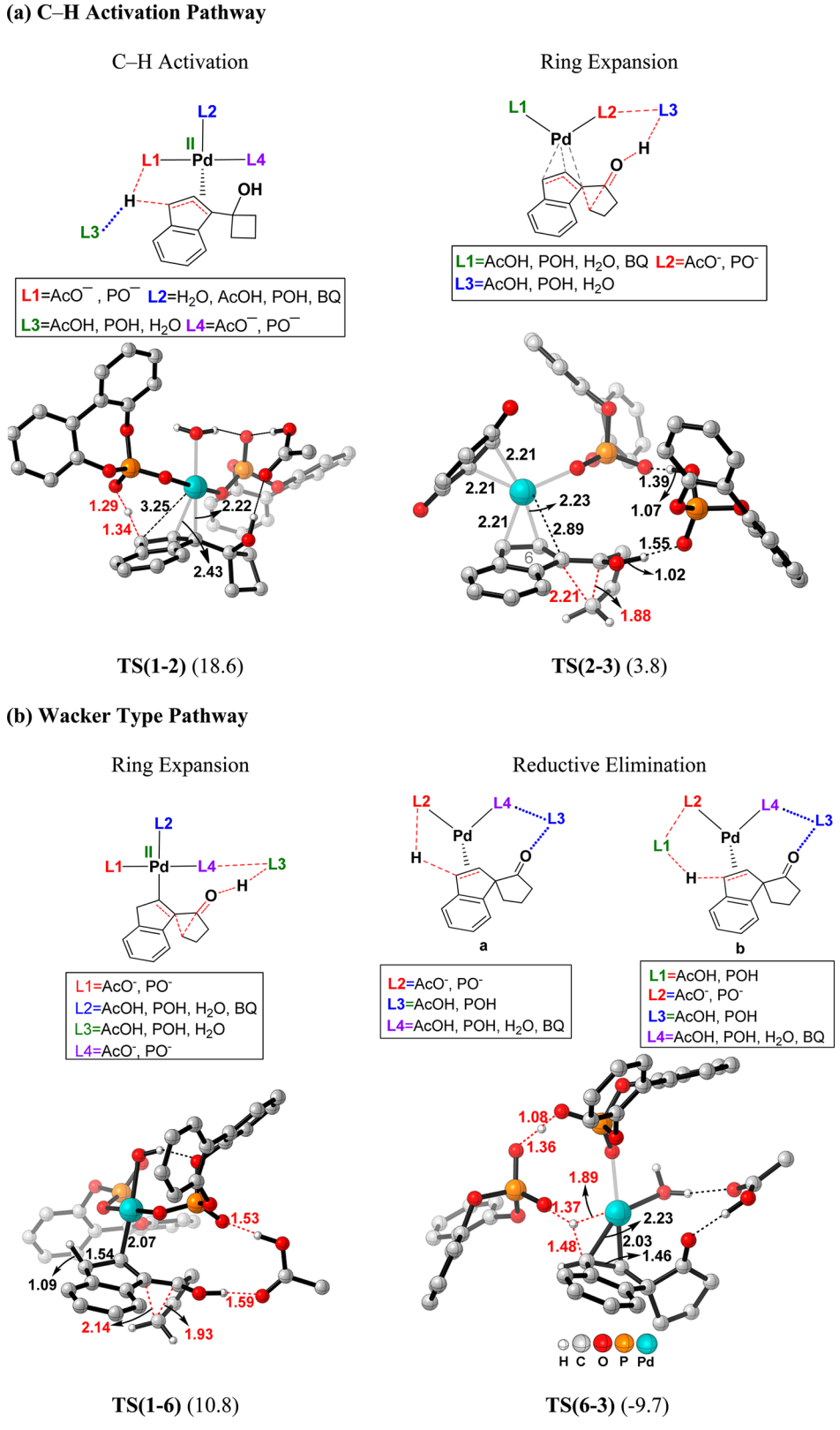

Figure 8. Different active species examined for the different steps involved in (a) the allylic C−H activation pathway and (b) Wacker-type process. Free energies of the lowest energy transition states (kcal/mol) at the $SMD_{toluene}$/M06/6-31G(d,p),LANL2DZ(Pd)//B3LYP/6-31G(d,p),LANL2DZ(Pd) level of theory are provided in parentheses. All distances are in angstroms.

diverse synthetic targets.[42] Asymmetric catalysis using dirhodium carbenoids typically uses chiral bridging ligands between rhodium atoms.[40a,43] However, there have been some recent and encouraging reports on the use of well-established achiral dirhodium carboxylates with an externally added axially chiral phosphoric acid as an additional catalyst under one-pot conditions (Scheme 8). Such strategies could help to steer the known catalytic reactions of dirhodium carbenoids in an

dx.doi.org/10.1021/cs501688y | ACS Catal. 2015, 5, 480−503

Table 1. Relative Free Energies (kcal/mol) at the $SMD_{toluene}$/M06/6-31G(d,p),LANL2DZ(Pd)//B3LYP/6-31G(d,p),LANL2DZ(Pd) Level of Theory for a Varying Number of Phosphate Ligands on Palladium

	allylic C−H activation		Wacker pathway	
no. of phosphate (PO^-) ligands on Pd	C−H activation	ring expansion	ring expansion	reductive elimination
zero (native)	36.0	20.3	30.5	9.2
one	26.7	10.3	21.5	−4.6
two	18.7	3.8	10.8	−13.2

Scheme 8. Asymmetric X−H (X = N, S) Insertion Reactions Catalyzed by Dirhodium Carboxylates and Chiral Spiro Phosphoric Acids (*R*)-SPA

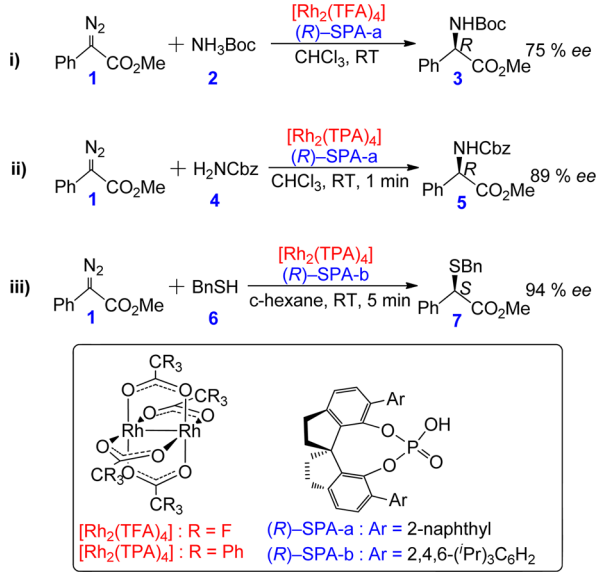

asymmetric fashion by introducing an additional source of chirality into the reaction medium.

In a very interesting study, Zhou and co-workers employed a carbene insertion strategy to make α-amino esters with enantioselectivities on the order of 95%.[44] The one-pot multicatalytic conditions used catalysts dirhodium(II) carboxylate and chiral spiro phosphoric acid ((*R*)-SPA) in the reaction between *tert*-butyl carbamate ($BocNH_2$) and α-diazo-α-phenylacetate (**1**), as shown in Scheme 8i. A similar reaction has also been carried out with $CbzNH_2$ (carboxybenzyl) using a similar approach depicted in Scheme 8ii. In this approach, the dirhodium carboxylate is an achiral catalyst and hence the chiral induction should be regarded as stemming from the chiral source, namely, spirophosphoric acid (*R*)-SPA. Similarly, Zhu, Yu, Zhao, and co-workers reported an S−H insertion reaction that made use of a cooperative catalytic protocol using a dirhodium carboxylate and a chiral SPA (Scheme 8iii).[45] The reactions shown in Scheme 8 appear to rely on cooperative/tandem catalysis offered by a chiral Brønsted acid on a dirhodium carbenoid platform.

In keeping with the current interest in multicatalytic reactions, there have been efforts to gain improved insight into the mechanism of the above-mentioned reactions as well. A few computational investigations have considered a generalized mechanism, as shown in Scheme 9. The origin of stereoselectivity in the reactions shown in Scheme 8 has been proposed to arise due to asymmetric protonation by (*R*)-SPA. The mechanism first involves the formation of a dirhodium carbene complex **2**. This further reacts with the nucleophile (R−XH) to form an ylide intermediate (**3**). Intermolecular proton transfer with a concomitant departure of the dirhodium catalyst can then give rise to an enol (**4**). A double proton transfer, as shown in **(4−5)**‡, wherein the phosphoric acid donates its proton to the prochiral carbon at

Scheme 9. General Mechanism for Asymmetric X−H (X = O, N, S) Insertion Reaction Catalyzed by Dirhodium Carbenoid in Conjuction with (*R*)-SPA

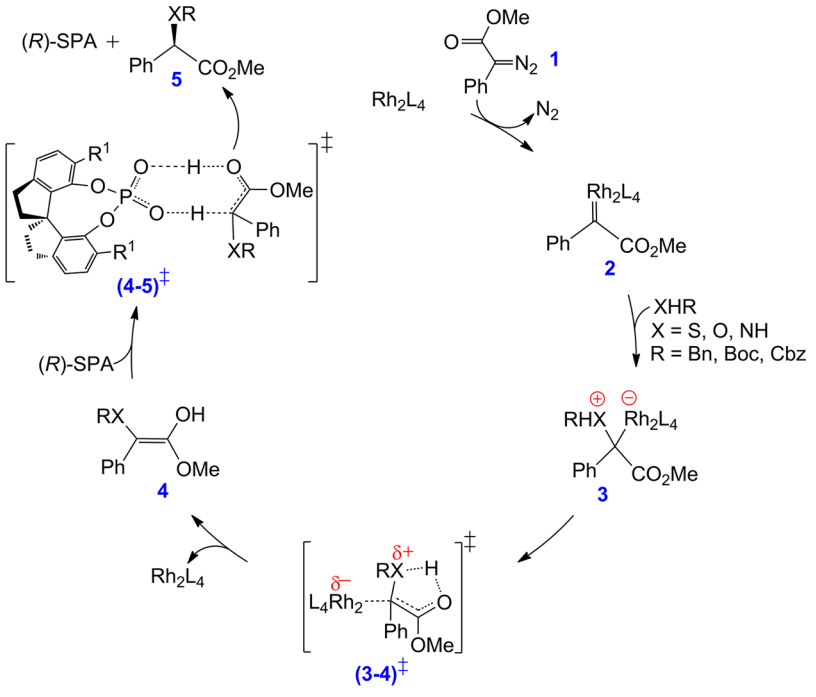

dx.doi.org/10.1021/cs501688y | ACS Catal. 2015, 5, 480−503

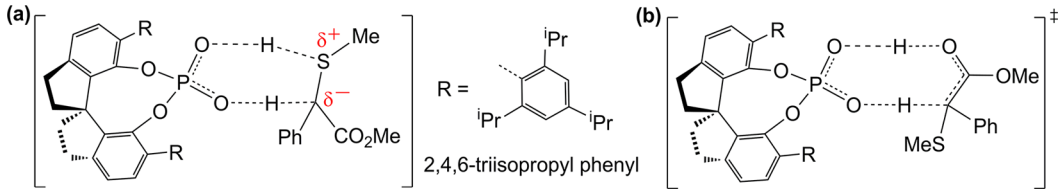

Figure 9. Different transition state models for an S−H insertion reaction.

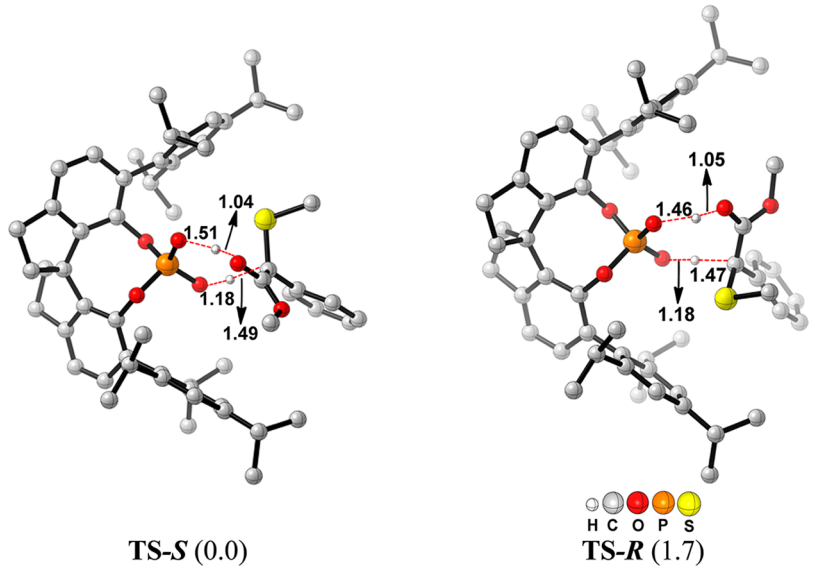

Figure 10. Stereodetermining transition states for the enol pathway for the S−H insertion reaction. Relative free energies (kcal/mol) at the M06-2X/6-31G(d)//B3LYP/6-31G(d) level of theory are provided in parentheses. All distances are in angstroms.

one end of **4** while it abstracts the enol proton from the other end, leads to final product **5**. While the mechanistic evidence tends to suggest some general similarities, substantial differences in the mode of proton transfer and the nature of intermediate involved in the stereocontrolling step, i.e., in $(\mathbf{4}-\mathbf{5})^{\ddagger}$, warrant additional discussion. For instance, in the case of dirhodium carboxylates, a potential ligand exchange between the bridging ligands on rhodium by the chiral phosphoric acid has been ruled out on the basis of ^{31}P NMR studies.[45] It can therefore be deduced that (*R*)-SPA does not coordinate to the metal but acts only as an outer-sphere Brønsted acid. However, there are other mechanistic ambiguities associated with this form of catalysis, particularly under cooperative catalytic conditions. The prime concern is the cooperativity between the two catalysts. In the generally proposed mechanism, as shown in Scheme 9, the dirhodium carboxylates and Brønsted acid act as catalysts in different steps of the reaction, suggesting a tandem catalysis as opposed to a cooperative mode. This is a significant question in light of the burgeoning recent developments in multicatalytic reactions.

The first DFT study was reported by Zhu, Yu, Zhou, and co-workers on an S−H insertion reaction, as shown in Scheme 8iii.[45] Two different transition state models differing in terms of the nature of the species involved in the stereoselectivity determining step were considered. The first model involves an ylide (Figure 9a), whereas the second one invokes participation of an enol (Figure 9b) in the stereocontrolling step. The enol model was found to be favorable over the ylide model by 9.4 kcal/mol at the B3LYP/6-311+G(d,p)//B3LYP/6-31G(d) level of theory. The difference in free energies between the transition states at the M06-2X/6-31G(d)//B3LYP/6-31G(d) level of theory was found to be 1.7 kcal/mol in favor of the *S* isomer, which is in agreement with the experimental observation. The optimized geometries of the stereodetermining transition states involved in the enol pathway are given in Figure 10. Steric repulsion between the tri-isopropyl group of the catalyst with the phenyl group of the enol was suggested to be the reason for the higher energy of **TS-*R***.

The transition state model proposed by Xie, Verpoort, Cao, and co-workers for an N−H insertion (Scheme 8ii) reaction is shown in Figure 11a. The key point to be noted is that only the enol intermediate was considered in the stereocontrolling step.[46] The origin of selectivity was attributed to the steric hindrance between the naphthyl group of the catalyst and the $CbzNH_2$ group of the enol, as shown in Figure 11b. In both the S−H and N−H insertion studies, the chiral spirophosphoric acid was considered to be participating only in the stereodetermining transition state in the form of a proton shuttle. Thus, it is likely that the authors intended to suggest a tandem mode of catalysis as opposed to a true cooperative catalytic system.

In the mechanistic studies presented thus far, the role of dirhodium catalyst has been confined to the generation of a dirhodium carbenoid intermediate in the early events of the reaction, prior to the stereocontrolling step. Very recently, Kisan and Sunoj have reported the mechanism and stereoselectivity of an asymmetric N−H insertion reaction (Scheme 8i).[47] These authors suggested a more realistic transition state model for the enantioselective protonation step by consider-

dx.doi.org/10.1021/cs501688y | ACS Catal. 2015, 5, 480−503

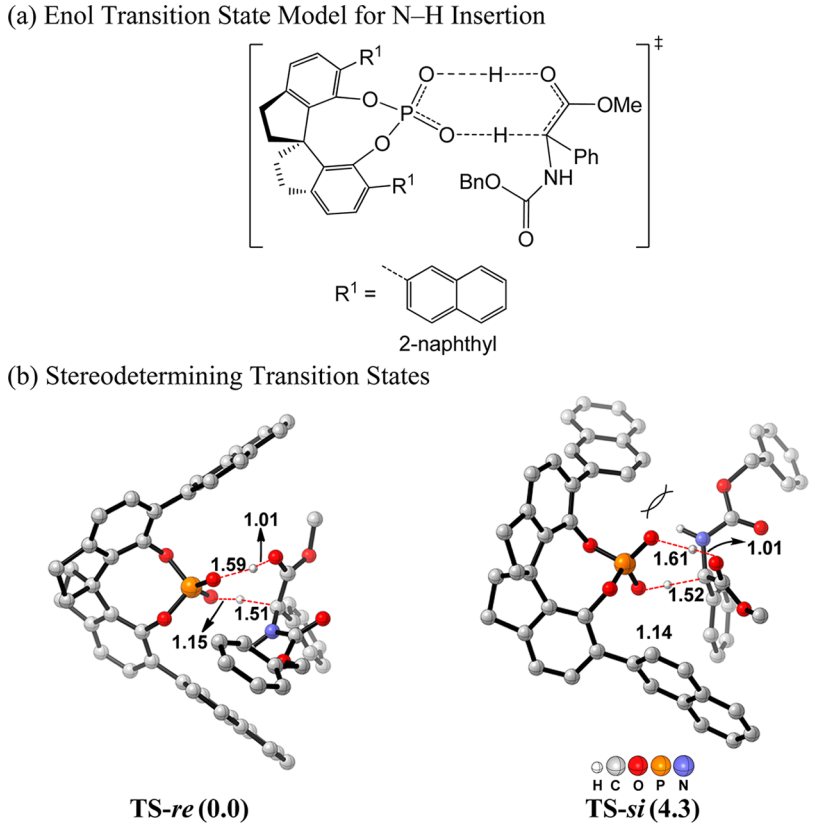

Figure 11. (a) Transition state model involving an enol intermediate and (b) stereodetermining transition states proposed for the N−H insertion reaction. Relative free energies (kcal/mol) at the $SMD_{chloroform}$/M06/6-31G(d),LANL2DZ(Rh)//B3LYP/6-31G(d),LANL2DZ(Rh) level of theory are provided in parentheses. Distances are given in angstroms.

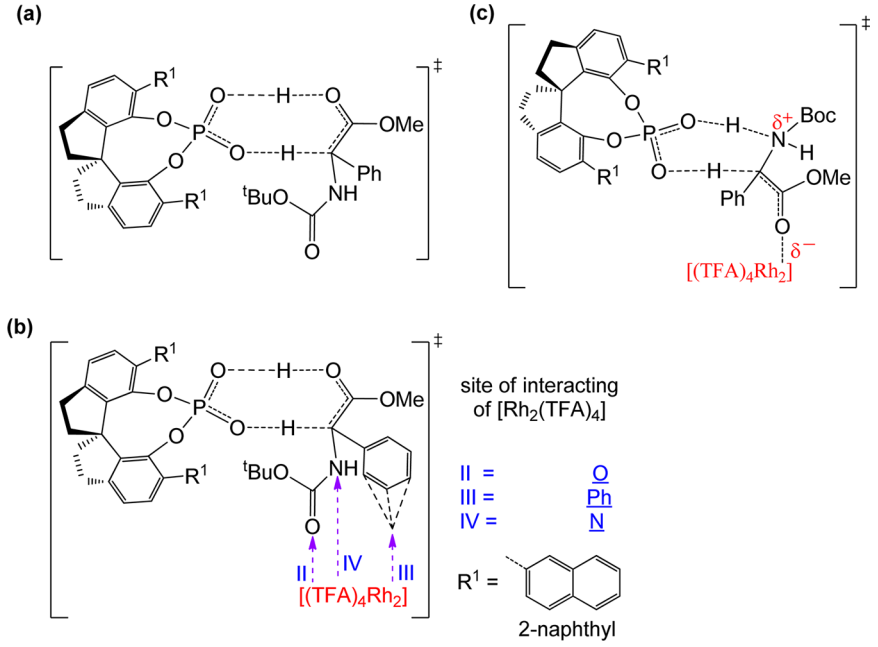

Figure 12. Stereocontrolling transition states involving a double proton transfer to (a) (*E*)-enol, (b) (*E*)-enol···$Rh_2(TFA)_4$, and (c) enolate.

ing the dirhodium acetate as being bound to the substrate, as shown in Figure 12b.

In addition to the participation of the enol intermediate (Figure 12a), the potential role of an enolate was also considered in the stereodetermining step (Figure 12c). The relative energies of the important transition states, provided in Table 2, indicate that the lowest energy transition state is the one in which the dirhodium acetate is bound to the carbonyl oxygen of the *N*-Boc group (entry 2 in Table 2, Figure 12b). Most importantly, the dirhodium bound enol was about 7 kcal/mol lower in energy compared to that in its absence. This was consistently the case for both the *si* or *re* prochiral

dx.doi.org/10.1021/cs501688y | ACS Catal. 2015, 5, 480−503

Table 2. Relative Gibbs Free Energies[a] of the Stereocontrolling Transition States Involving a Relay Proton Transfer by (*R*)-SPA Obtained at the $SMD_{chloroform}$/M06/LANL2DZ(Rh),6-31G(d,p)//B3LYP/LANL2DZ(Rh),6-31G(d) Level of Theory

entry	intermediate	*si* face	*re* face	predicted enantiomer
1	Enol	−17.3	−12.4	*R*
2	Enol O···$Rh_2(TFA)_4$	−24.4	−17.0	*R*
3	Enol Ph···$Rh_2(TFA)_4$	−20.9	−15.8	*R*
4	Enol N···$Rh_2(TFA)_4$	−9.4	−12.7	*S*
5	Enolate ((*Z*)-enolate)	−14.2	−10.7	*R*
6	Enolate ((*E*)-enolate)	−12.1	−12.6	*S*

[a]In kcal/mol, with respect to the separated reactants. The site of coordination of dirhodium catalyst is emphasized by being underlined.

face of the enol protonation. Another important difference was that the Gibbs free energies of the transition state for the enantioselective protonation of the commonly proposed dirhodium enolate intermediate (Figure 12c) by (*R*)-SPA is higher by about 10 kcal/mol than in the corresponding dirhodium enol pathway (entries 5 and 6 versus 2 in Table 2). The above-mentioned mechanistic features evidently suggest that a cooperativity between both catalysts, dirhodium and (*R*)-SPA, is operating in the stereocontrolling step of the reaction. In other words, cooperativity between two catalysts by way of its participation in the stereocontrolling step of the reaction is conspicuous.

The authors also described the process of asymmetric induction through the analyses of the nature of interactions in the transition states for the stereoselective protonation. In particular, a transition state model wherein $Rh_2(TFA)_4$ is bound to the carbonyl oxygen of the substrate (7O···$Rh_2(TFA)_4$) was described in both the gas and condensed phases. The chiral (*R*)-SPA was noted as remaining closer to the developing stereocenter, as shown in **TS-*re*** and **TS-*si*** in Figure 13, such that the transfer of chirality is more effective. Other vital, weak nonbonding interactions in the transition state, N−H···π and C−H···π, are shown in Figure 13 as a and b. Interestingly, these interactions are relatively shorter in lower energy **TS-*si*** than in **TS-*re***. Similarly, the hydrogen bonding between the CF_3 groups of the dirhodium bridging ligand and the C−H bonds of the binaphthyl (c to g) is also better in **TS-*si*** as compared to that in **TS-*re***. In addition to the energetic advantage presented earlier, these structural features also confirm that both catalysts participate cooperatively in the enantioselective protonation.

Transition Metal−NHC Cooperative Catalysis. As with other organocatalysts, NHCs have also been successfully employed in multicatalytic reactions. The use of NHCs as asymmetric organocatalysts has been amply demonstrated over the past decade.[15] NHCs have also found applications in the form of ligands bound to transition metals.[48] In 2008, the Glorius group reported the compatibility of NHC to act both as a ligand bound to a palladium catalyst and as an independent catalyst, perhaps acting as an organocatalyst, in a multicomponent coupling reaction.[49] It was proposed that since NHC catalyst was used in excess it can bind to the metal center and also act as a free catalyst.

Over the years, it has been established that NHCs can form strong bonding with late transition metals, whereas it can paricipate in weaker interaction with early transition metals. The latter attribute has recently been exploited in the domain of cooperative catalysis using NHC.[50] For example, in 2010, Scheidt and co-workers demonstrated a cooperative catalytic approach involving NHC and a Lewis acid.[15l] They employed a triazolium-derived NHC in conjunction with $Mg(O^tBu)_2$ for an enantioselective addition of homoenolate equivalents to *N*-benzoyl hydrazones. It was proposed that the mode of action of catalysts relies on lowering the HOMO−LUMO gap between the participating reactants. Even though there have been several examples of metal−NHC cooperative catalytic systems, there have been only a few mechanistic studies reported to date.

Domingo and co-workers carried out a DFT investigation of a NHC and Lewis acid (LA) catalyzed annulation reaction (Scheme 10).[51] The role of $Ti(Oi\text{-}Pr)_4$ was investigated by using DFT(B3LYP) methods. The mechanism of the reaction was first investigated in the absence of the LA and subsequently in its presence to establish the actual role of the Lewis acid.

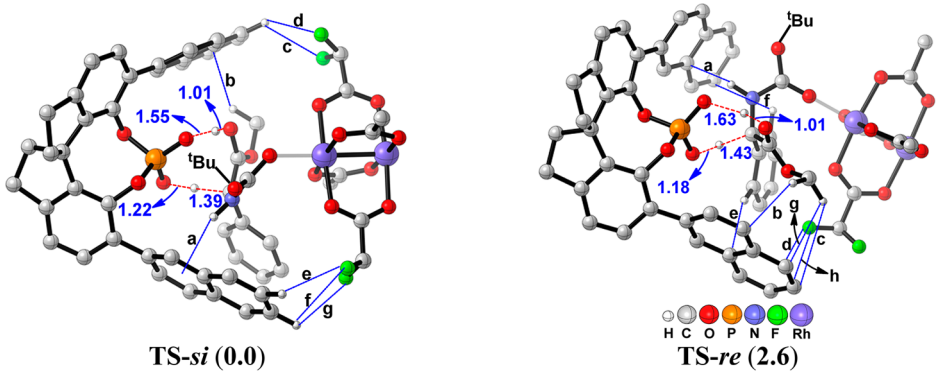

	a	b	c	d	e	f	g	h
***si*-TS**	2.41	2.69	2.68	2.69	2.86	3.00	2.83	-
***re*-TS**	2.59	2.64	2.96	3.38	2.96	3.07	2.96	3.00

Figure 13. Optimized geometries of the stereocontrolling transition states for the enantioselective protonation of the α-carbon of the enol (Enol O···[$Rh_2(TFA)_4$]) by (*R*)-SPA optimized at the $SMD_{chloroform}$/M06/LANL2DZ(Rh),6-31G(d,p) level of theory. The relative Gibbs free energy difference between two diastereomeric transition states is provided in parentheses. Distances are in angstroms. Only selected C, H, and F are shown.

dx.doi.org/10.1021/cs501688y | ACS Catal. 2015, 5, 480−503

Scheme 10. NHC and Lewis Acid (LA) Catalyzed Annulation Reaction between an Enal and an Enone

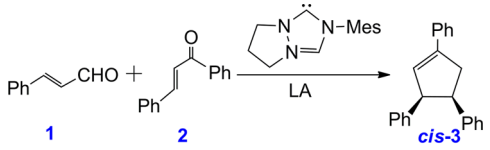

Entry	LA (equiv)	% yield	*cis* : *trans*
1	-	*73*	1:3
2	$Zn(OTf)_2$	*0*	-
3	$Mg(OTf)_2$	*0*	-
4	$Ti(Oi\text{-}Pr)_4$	47(71)[a]	20:1

The authors were able to establish the energetic advantage in the Lewis acid-assisted pathway as well as to rationalize the observed diastereoselectivity. The computed energetics at the $PCM_{dichloromethane}$/B3LYP/6-31G(d,p) level of theory are provided in Scheme 11. It can be clearly seen that the energies of the transition states involved in the LA-assisted pathway (shown in blue) are considerably lower than that in the unassisted one (shown in red) throughout the catalytic cycle.

Rationalization of the experimentally observed diastereoselectivity was done by using the computed energetics, as summarized in Schemes 12 and 13. In the absence of a LA, the major product was noted to be *trans*, whereas in the presence of LA, the formation of a *cis* product occurred predominantly. The formation of the *trans* product via **TS6** was 3.5 kcal/mol higher in energy than the formation of *cis* product via **TS5**. In the absence of the LA, the formation of the *trans* product via **TS8** was found to be energetically favored over that of the *cis* product (via **TS7**) by 2.4 kcal/mol. Moreover, the activation barrier for the formation of *cis* product via **TS5** was 3.7 kcal/mol lower than that for the formation of the *trans* product in the unassisted pathway via **TS8**. It should be noted that even though **TS5** experiences greater steric interactions due to the parallel arrangement between the reacting partners (**4** and **2**) it was of lower energy than **TS6**. The parallel arrangement of **4** and **2** in **TS5** as opposed to the twisted arrangement in **TS6** was suggested to be responsible for a greater charge transfer in **TS5**. This, consequently, leads to a lowering of the energy of **TS5**, leading to the *cis* product (**8**), in comparison to **TS6**, which yields the *trans* product (**11**). The computed energetics and the predicted stereochemical outcome were found to be in good agreement with the experimental observations. Similar to the earlier examples discussed in this review, the action of two catalysts is evident even in this example, suggesting a synergetic participation in the key catalytic events. Hence, this reaction also constitutes an interesting example of organo–transition metal cooperative catalysis.

Transition Metal–Cinchona Alkaloid Cooperative Catalysis. Amines have received an unprecedented attention in the past decade owing to their popularity as effective organocatalysts.[13] Along a similar line, the chiral and achiral variants of transition metal–amine cooperative catalysis have also grown considerably in recent years.[52] Amines are known to activate a range of aldehydes/ketones in the form of an enamine or iminium species. In addition to the use of primary and secondary amines, tertiary amines have also found interesting applications in multicatalytic reactions, mainly in the form of Lewis bases. Cinchona-type catalysts have been used individually as successful organocatalysts for a range of different reactions.[13] Cooperative catalytic systems comprising metals and cinchona-based scaffolds have also been developed to carry out the synthesis of various complex molecules.[53]

Ibrahem, Córdova, and co-workers used a copper salt and chiral amine catalytic system for an enantioselective conjugate addition of a dimethylsilanyl group to α,β-unsaturated compounds for the formation of β-silylaldehyde product **8** (Scheme 14).[54] The authors carried out DFT(B3LYP) computations on a model system to identify the nature of the ligand (L = chloride, *p*-nitrobenzoate, pyrrolidine). The mechanism is suggested to involve the formation of a $PhMe_2SiCuL$ (**5**) species first (Scheme 15). Chloride is found to be the most preferred ligand for the silylation step. There are two key events in the catalytic cycle: the first is the activation of the enal (**2**) by the secondary amine catalyst, and the second is a copper-catalyzed silylation. The iminium cation (**3**) formed between the chiral amine and the enal interacts with the copper complex (**5**) to yield intermediate **6**. The next step involves stereoselective C–Si bond formation, resulting in intermediate **7**. The most important point is that both the chiral amine and the transition metal participate in the stereoselective step, thereby indicating cooperativity between the organo and metal catalysts.

To probe the origins of stereoselectivity, stereocontrolling transition states were located using DFT(B3LYP) methods. The optimized transition state geometries, as given in Figure 14, convey that in the lower energy **TS-*re*** the attack of the nucleophile (silyl moiety) occurs at the *re* face of the iminium ion, which is not shielded by the bulky α-substituent

Scheme 11. Formation of the Extended Ti(IV)–Breslow Intermediate (4) and the Breslow Intermediate (6) in the Absence of Ti(IV)[a]

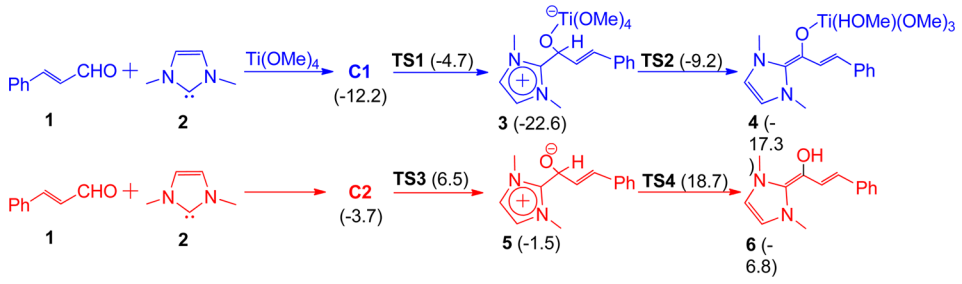

[a]Relative free energies (kcal/mol) with respect to the separated reactants at the $PCM_{dichloromethane}$/B3LYP/6-31G(d,p)//B3LYP/6-31G(d,p) level of theory are given in parentheses.

dx.doi.org/10.1021/cs501688y | *ACS Catal.* 2015, 5, 480–503

Scheme 12. Formation of *Cis* (8) and *Trans* (11) Products in the Presence of Lewis Acids[a]

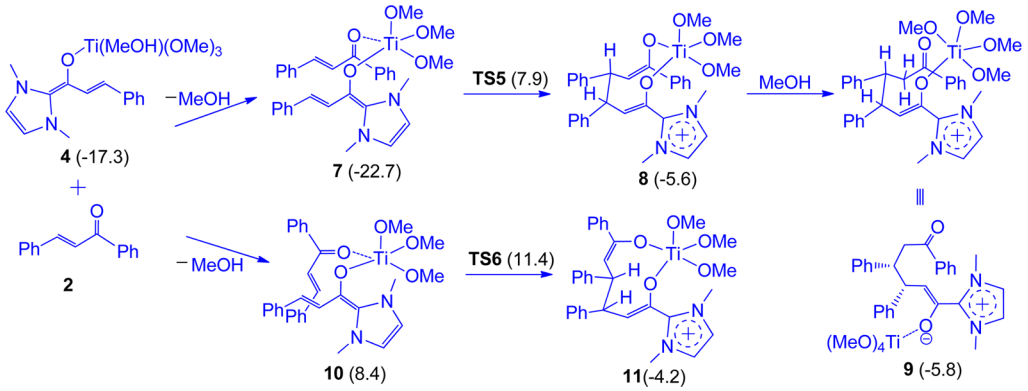

[a]Relative free energies (kcal/mol) with respect to the separated reactants at the $PCM_{dichloromethane}$/B3LYP/6-31G(d,p)//B3LYP/6-31G(d,p) level of theory are given in parentheses.

Scheme 13. Formation of *Cis* (13) and *Trans* (15) Products in the Absence of Lewis Acids[a]

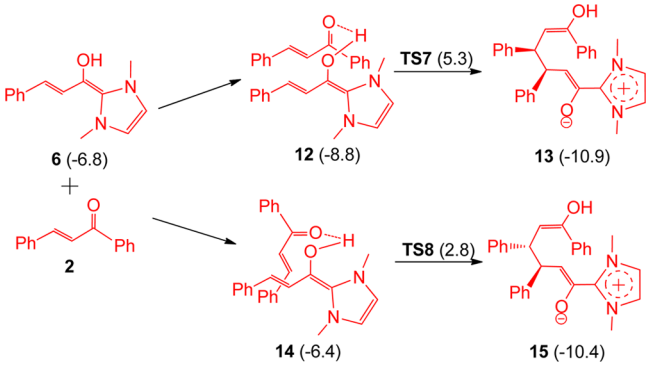

[a]Relative free energies (kcal/mol) with respect to the separated reactants at the $PCM_{dichloromethane}$/B3LYP/6-31G(d,p)//B3LYP/6-31G(d,p) level of theory are given in parentheses.

Scheme 14. Addition of a Silyl Group to an α,β-Unsaturated Aldehyde Catalyzed by a Cu Salt and a Chiral Amine

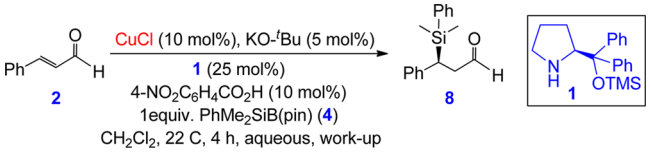

(phenyldimethylsilyl group) on the pyrrolidine ring. However, in the higher energy **TS-*si***, the nucleophile approaches from the same face as that of the bulky group, resulting in considerable steric interactions. Thus, steric interactions between the transition metal catalyst and the organocatalyst were suggested to be the origin of the predicted stereoselectivity.

In another recent report, Patil, Datta, and Nijamudheen examined the cooperativity between pyrrolidine and Cu in a condensation reaction between an aminoaldehyde and an alkyne by using DFT(B3LYP) computational tools.[55] The reaction, as shown in Scheme 16, involves the condensation of **1** and **2**. It was proposed that cooperative action between Cu and pyrrolidine catalysts leads to 6-*endo* (**3**) and 5-*exo* (**3′**) cyclized products.

The authors first considered the formation of an iminium ion between 2-aminobenzaldehyde (**1**) and pyrrolidine. This iminium ion subsequently reacts with the alkyne (**2**) in the presence of CuI to give an aminoalkyne intermediate (**4**), which, upon uptake of a CuI molecule, yields complex **5** (Scheme 17). This complex subsequently undergoes cyclization to give intermediate **6** via an *endo-dig* pathway. The next step involves proton abstraction by an explicit molecule of pyrrolidine to furnish intermediate **7**. The final step involves the formation of intermediate **8** via a protodemetalation step. On the basis of the computed Gibbs free energy profile, it was suggested that the formation of the *endo* product was favored over the *exo* product. It is equally important to note that both Cu and pyrrolidine catalysts participate together in the catalytic cycle, in line with other examples of cooperative catalysis presented in this review.

In another important example, Paton, Dixon, and coworkers employed both DFT(M06-2X) and experimental (kinetic, isotopic labeling, nonlinear effects, and titration experiments) methods to establish the mechanism of a Conia-ene reaction of β-ketoester tethered with an alkyne.[56] The reaction is catalyzed by a cooperative catalytic system comprising Cu and cinchona-derived amino urea catalysts (Scheme 18i).

The first step in the catalytic cycle, as shown in Scheme 18ii, involves the enolization of the alkyne-tethered β-ketoester (**2**), leading to the formation of a Cu-enolate (**3**). The enolate subsequently forms a complex (**4**) with the cinchona-derived organocatalyst (**1**). The conversion of **4** to **5** involving carbocyclization with a concomitant release of **1** was proposed to be the stereodetermining step of this reaction. It was noted that both transition metal (Cu) and organocatalyst (**1b**) participate in the rate-determining step (enolization) as well as in the stereodetermining step (*syn*-carbocupration). Catalyst **1** ligates to Cu via its quinuclidine N and promotes the enolization step. A similar kind of ligation was also observed in the stereodetermining step. Thus, both catalysts act cooperatively in the important steps of the catalytic cycle.

The optimized geometries of the stereodetermining transition states are shown in Figure 15. The energy difference of 1.3 kcal/mol between the diastereomeric transition states leads to an *ee* of 82%, which is in accord with the experimental value of 92%. In both transition states, Cu holds the substrate through interaction with the β-dicarbonyl enolate and the alkyne group. However, in the

dx.doi.org/10.1021/cs501688y | ACS Catal. 2015, 5, 480−503

Scheme 15. Mechanism for the Conjugate Addition of Dimethylsilanyl Group to *α,β*-Unsaturated Aldehyde

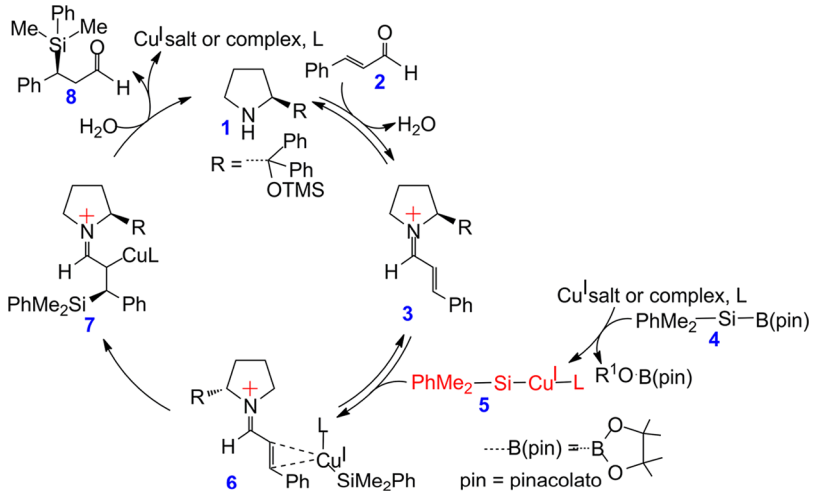

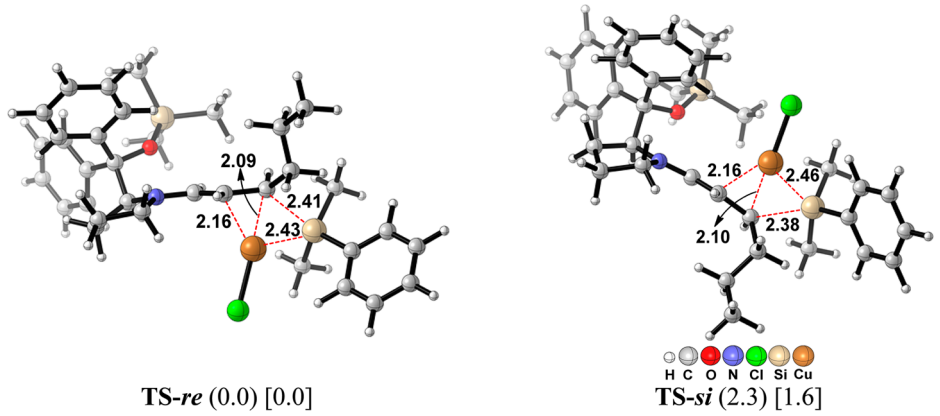

TS-*re* (0.0) [0.0] **TS-*si*** (2.3) [1.6]

Figure 14. Stereodetermining transition states for C−Si bond formation. Relative free energies (kcal/mol) at the $CPCM_{dichloromethane}$/B3LYP/6-311+G(2d,2p)//B3LYP/6-31G(d),LANL2DZ(Cu) level of theory are provided in parentheses. All distances are in angstroms.

Scheme 16. Cu/Pyrrolidine Catalyzed Condensation of Aminoaldehyde and Alkyne

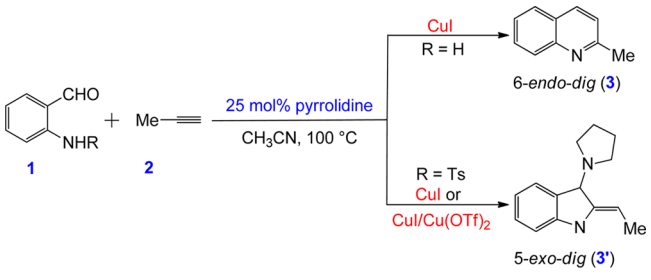

lower energy transition state, an additional interaction was noted between the ester O and Cu (2.34 Å), rendering additional stabilization to the lower energy **TS-*re***. Another important difference to account for the difference in energy is the H-bonding between the enolate and the thiourea moiety of the organocatalyst. In the lower energy **TS-*re***, the ketonic oxygen engages in a hydrogen-bonding interaction (1.86 and 2.04 Å) with the urea moiety of the organocatalyst while maintaining its coordination to Cu (2.29 Å). However, in the higher energy transition state, the ester O is involved in H-bonding (2.01 and 1.85 Å), which results in decoordination from the Cu center.

COMPUTATIONAL STUDIES ON COOPERATIVITY BETWEEN TWO ORGANOCATALYSTS

As described in the previous sections, Brønsted acids, NHCs, and amines are highly successful organocatalysts used to carry out various synthetic transformations. The different combinations that can arise by combining them to form cooperative systems are akin to that in metal−organo cooperative catalysis. Jacobsen and co-workers reported the Povarov reaction catalyzed by nitrobenzenesulfonic acid and chiral urea/thiourea.[57] The reaction involves a [4 + 2] cycloaddition of *N*-aryl imines and electron-rich olefins to yield tetrahydroquinoline derivatives with three contiguous stereocenters, as shown in Scheme 19.

The authors considered the following key steps in their mechanism. Initially, the *N*-aryl imine and the Brønsted acid react to form an iminium ion and a conjugate base of sulfonic acid. This ion pair, denoted as **5** as shown in Figure 16), then reacts with the olefin to give the cycloadduct ($\mathbf{4}_{exo}$) via transition state **TS(5−4$_{exo}$)**. In this stereocontrolling transition state, the conjugate base was found to form H-bonds to the iminium ion as well as with the NH group of the urea moiety. Such a hydrogen-bonding network was suggested to be the responsible factor holding the substrate and the urea catalyst together, as shown in the lowest energy **TS(5−4$_{exo}$)** in Figure 16. A comparison between the diastereomeric transition states

dx.doi.org/10.1021/cs501688y | *ACS Catal.* 2015, 5, 480−503

Scheme 17. Free Energy Profile (kcal/mol) at the B3LYP/6-31+G(d),LANL2DZ(Cu,I) Level of Theory for the Formation of 6-*Endo-dig* and 5-*Exo-dig* Products from the Aminoalkyne

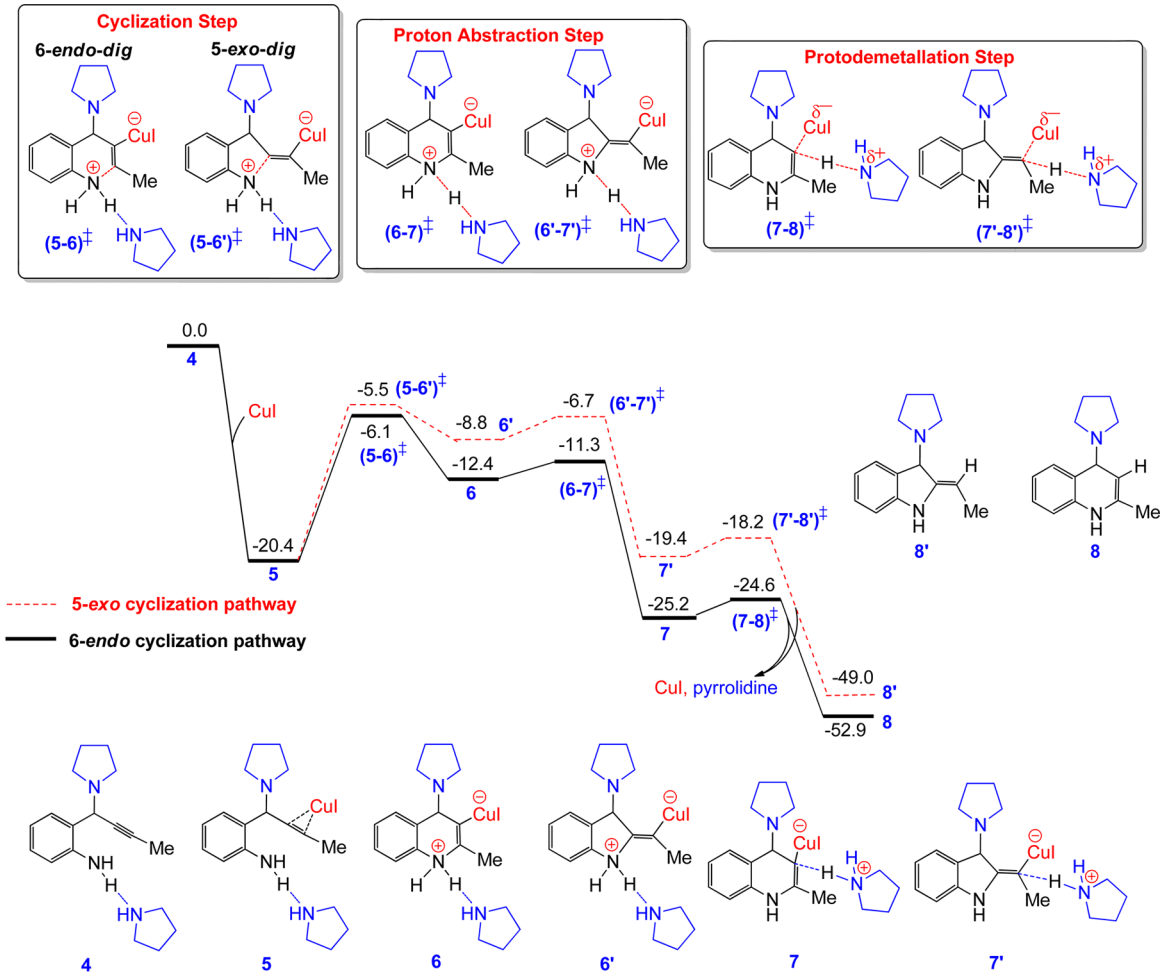

revealed that the lower energy **TS(5−4$_{exo}$)** exhibits additional $\pi\cdots\pi$ interactions between the aryl group of the catalyst and the iminium ion, contributing to its enhanced stability by 3.6 kcal/mol at the M05-2X/6-31+G(d,p)//B3LYP/6-31G(d) level of theory (Figure 16). It can be readily noticed that in the stereocontrolling transition state both catalysts (urea and nitrobenzenesulfonic acid) cooperatively participate to enable adequate stereoselectivity.

Schreiner and co-workers reported another study involving thiourea−Brønsted acid catalytic system for the cyanosilylation of aldehydes (Scheme 20).[58] A hydrogen-bonded complex **A** having an *E,Z* orientation of the N−H protons of thiourea catalysts **1a**, as shown in Figure 17, was proposed on the basis of NMR and mass spectrometry studies carried out with catalyst **1a** and dimethylbenzoic acid. The change in chemical shift with a change in the amount of the acid confirmed the interaction between the two organocatalysts. Geometry optimization of complex **1a** and benzoic acid (**4**) at the M06/6-31G(d) level of theory resulted in two lower energy minima, **A** and **B**, with *E,Z* and *Z,Z* orientations, respectively (Figure 17). The Gibbs free energy difference between these two complexes was found to be 2.2 kcal/mol in favor of complex **A**. This complex, with *E,Z* orientation of the N−H protons, was suggested to engage with the benzoic acid through two H-bonding interactions, such as N−H···O═C (2.02 Å) and N···H−O (1.71 Å). The ternary complex, **C**, involving **A** and the aldehyde is shown in Figure 17. The aldehyde forms a hydrogen bond (2.08 Å) with the N−H group of the thiourea catalyst, which does not engage in H-bonding with the Brønsted acid. Additionally, a T-shaped C−H···π interaction (2.71 Å) between the phenyl ring of the aldehyde and the ortho H of the thiourea was also identified. It can be clearly seen that both catalysts (chiral thiourea and dimethylbenzoic acid) cooperatively participate in the formation of the ternary complex **C**. Such chiral recognition is expected to facilitate stereoinduction in this example.

Through this review, we have tried to bring forth a series of examples wherein transition state modeling has been successfully employed toward gaining vital molecular insights into cooperative catalysis. The utility of a transition state model and its success, particularly in an increasingly complex scenario such as that in cooperative catalysis, would certainly owe, in part, to the technical soundness. Assuming that the choice of computational methodology is adequate, potential pitfalls in transition state models due to inadequate sampling of the large conformational space as well as different mechanistic pathways can be dangerous. While conformational search methods are readily available for ground-state molecules, such approaches for transition states are relatively scarce. Most force field based searches are not quite effective in dealing with bond-breaking and -forming processes. Ab initio molecular dynamics methods, on the other hand, appear

dx.doi.org/10.1021/cs501688y | ACS Catal. 2015, 5, 480−503

Scheme 18. (i) Cu−Cinchona Catalyzed Conia-ene Reaction and (ii) the Mechanism of Cyclization of β-Ketoester Tethered with an Alkyne

(i) Cu-cinchona catalyzed Conia-ene reaction of β-ketoester tethered with an alkyne

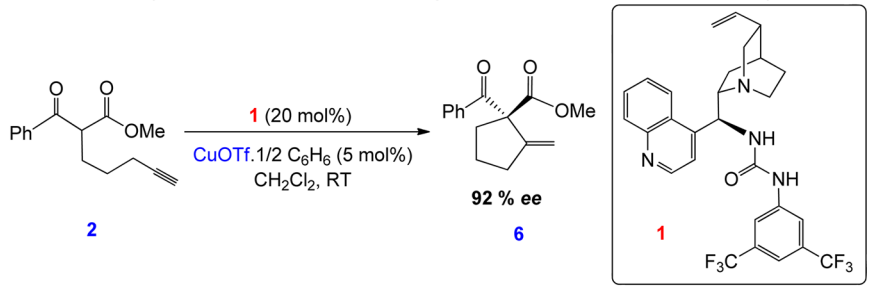

(ii) Mechanism of cyclization of alkyne linked β-ketoester

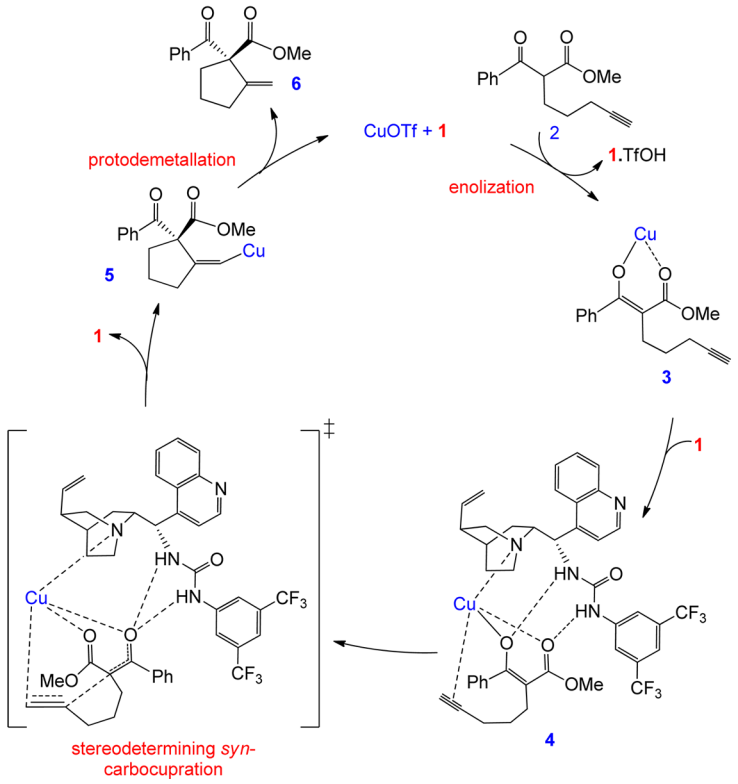

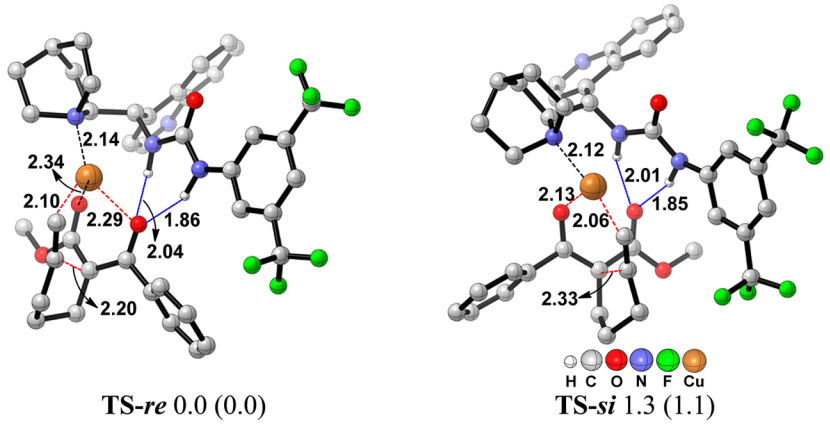

TS-*re* 0.0 (0.0) **TS-*si* 1.3 (1.1)**

Figure 15. Stereodetermining transition states for C−C bond formation leading to **5** at the M06-2X/6-31G(d) level of theory. The relative energies (kcal/mol) inclusive of ZPE correction are provided at the M06-2X/6-31G(d) level of theory, and that at the M06-2X/6-311+G(d,p) level of theory is in parentheses. All distances are in angstroms.

dx.doi.org/10.1021/cs501688y | ACS Catal. 2015, 5, 480−503

Scheme 19. Sulfonic Acid−Thiourea-Catalyzed Povarov Reaction

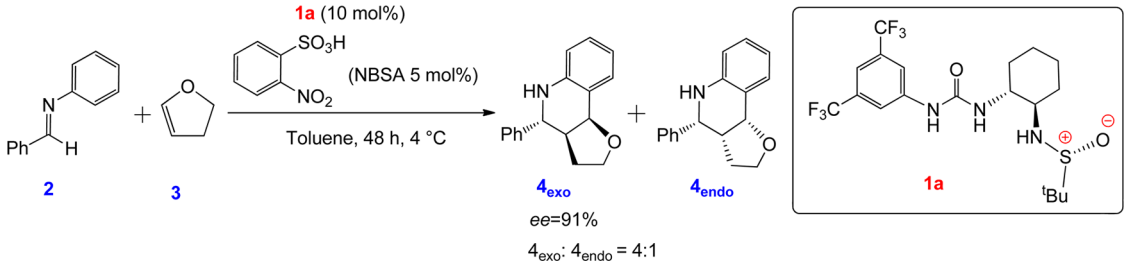

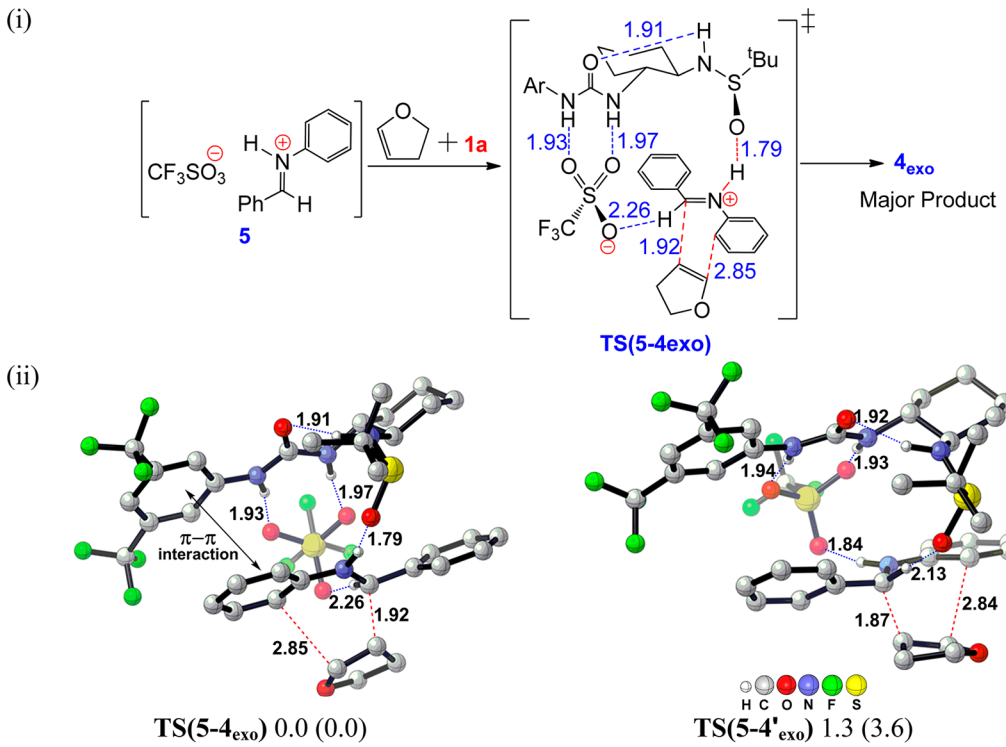

Figure 16. (i) Ion pair **5** and its reaction with the olefin in the presence of **1a** to give the major product $\mathbf{4}_{exo}$ and (ii) the diastereomeric transition states **TS(5−4$_{exo}$)** and **TS(5−4′$_{exo}$)**. The electronic energies (kcal/mol) at the B3LYP/6-31G(d) level of theory are given. The values in parentheses correspond to the energies at the M05-2X/6-31+G(d,p)//B3LYP/6-31G(d) level of theory. All distances are in angstroms.

Scheme 20. Thiourea−Benzoic Acid Catalyzed Cyanosilylation of Aldehydes

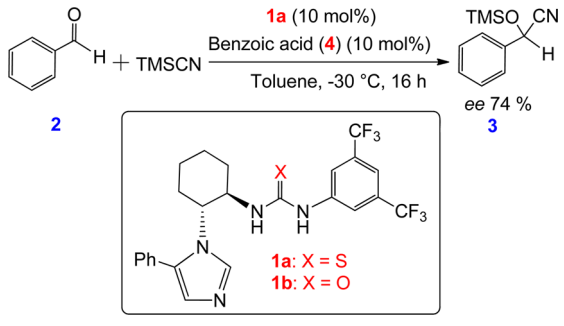

to enjoy only limited acceptance compared to that for stationary-state electronic structure approaches. Sampling different conformers of a given configuration (wherein the relative connectivity between the catalysts and substrates are maintained) is itself a formidable challenge due to the larger number of rotatable bonds typically found in the chiral catalysts and the reacting substrates. Changes in configuration, arising due to the differences in ligand disposition, are expected to further compound the problem of locating the most preferred transition state geometry. By and large, these issues have been addressed by using chemically intuitive configurational and conformational sampling in the stereo-controlling transition states. However, automated search algorithms are now becoming available that could address these issues more effectively.[59] Again, the suitability of such methods is limited because the availability is not very encouraging at this stage.

SUMMARY AND OUTLOOK

Methodological developments to make use of the complementary catalytic abilities of different catalysts under one-pot reaction conditions have witnessed steady growth over the past few years. In view of the latent promise that the area of cooperative catalysis holds, the effort directed toward deciphering this relatively complex mechanistic manifold should be regarded as timely and important. Through this review, we have chosen a subset of examples wherein computational tools have been meticulously applied toward

dx.doi.org/10.1021/cs501688y | ACS Catal. 2015, 5, 480−503

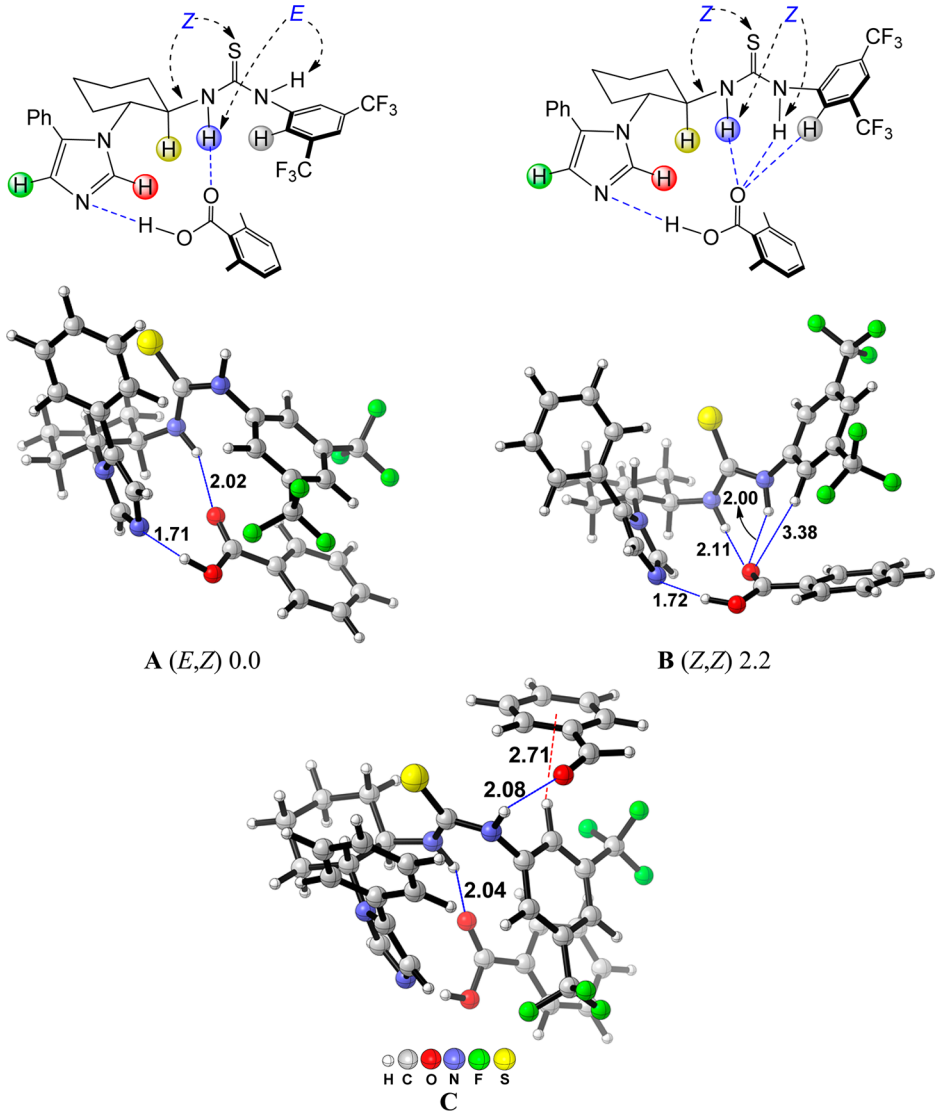

Figure 17. Hydrogen-bonded complex **A** (*E*,*Z* orientation), **B** (*Z*,*Z* orientation) (**1a** and dimethylbenzoic acid), and **C** (**1a**, dimethylbenzoic acid and benzaldehyde) optimized at the M06/6-31G(d,p) level of theory. The relative Gibbs free energies are in kcal/mol. All distances are in angstroms.

gaining vital molecular insights in understanding the origin of cooperativity. As the process of catalysis, in particular asymmetric catalysis, pivotally depends on the stereoelectronic features as well as on the energetics of transition states, it has been our aim to emphasize examples reporting transition state modeling in cooperative catalysis. The majority of examples belong to cooperative catalysis involving transition metals and organocatalysis. The mode of interaction between the catalysts and substrates has been a point of discussion in order to bring sufficient molecular level understanding. We believe that the present-day transition state models are indeed a good beginning toward understanding a complex catalytic scenario. Incorporation of various additives, oxidants, and explicit solvents as well as other environmental parameters into the transition state models will become available in more refined models in the near future. Arriving at a rational and generalized framework for understanding cooperative asymmetric catalysis will follow in the coming years.

AUTHOR INFORMATION

Corresponding Author

*E-mail: sunoj@chem.iitb.ac.in.

Notes

The authors declare no competing financial interest.

ACKNOWLEDGMENTS

G.J. and H.K.K acknowledge senior research fellowship from the Council of Scientific and Industrial Research (CSIR-New Delhi).

REFERENCES

(1) (a) Scheffler, U.; Mahrwald, R. *Chem.—Eur. J.* **2013**, *19*, 14346−14396. (b) Maruoka, K.; List, B.; Yamamoto, H.; Gong, L.-Z. *Chem. Commun.* **2012**, *48*, 10703−10703. (c) List, B.; Yang, J. W. *Science* **2006**, *313*, 1584−1586. (d) Mukherjee, S.; Yang, J. W.; Hoffmann, S.; List, B. *Chem. Rev.* **2007**, *107*, 5471−5569. (e) MacMillan, D. W. C. *Nature* **2008**, *455*, 304−308. (f) Bertelsen, S.; Jørgensen, K. A. *Chem. Soc. Rev.* **2009**, *38*, 2178−2189. (g) Dondoni, A.; Massi, A. *Angew. Chem., Int. Ed.* **2008**, *47*, 4638−4660. (h) Barbas, C. F. *Angew. Chem., Int. Ed.* **2008**, *47*, 42−

47. (i) Melchiorre, P.; Marigo, M.; Carlone, A.; Bartoli, G. *Angew. Chem., Int. Ed.* **2008**, *47*, 6138−6171. (j) Ryan, S. J.; Candish, L.; Lupton, D. W. *Chem. Soc. Rev.* **2013**, *42*, 4906−4917. (k) Doyle, A. G.; Jacobsen, E. N. *Chem. Rev.* **2007**, *107*, 5713−5743. (l) Volla, C. M. R.; Atodiresei, I.; Rueping, M. *Chem. Rev.* **2014**, *114*, 2390−2431.
(2) (a) Desimoni, G.; Faita, G.; Jørgenson, K. A. *Chem. Rev.* **2011**, *111*, PR284−PR437. (b) Hawner, C.; Alexakis, A. *Chem. Commun.* **2010**, *46*, 7295−7306. (c) *Comprehensive Asymmetric Catalysis and Supplements 1 and 2*; Jacobsen, E. N., Pfaltz, A., Yamamoto, H., Eds.; Springer: New York, 2004. (d) Trost, B. M.; Crawley, M. L. *Chem. Rev.* **2003**, *103*, 2921−2944. (e) Lu, Z.; Ma, S.-M. *Angew. Chem., Int. Ed.* **2008**, *47*, 258−297. (f) Chen, M. S.; White, M. C. *Science* **2007**, *318*, 783−787. (g) Wu, X.-F.; Fang, X.; Wu, L.; Jackstell, R.; Neumann, H.; Beller, M. *Acc. Chem. Res.* **2014**, *47*, 1041−1053. (h) Liu, X.; He, L.; Liu, Y.-M.; Cao, Y. *Acc. Chem. Res.* **2014**, *47*, 793−804. (i) Xiao, Q.; Zhang, Y.; Wang, J. *Acc. Chem. Res.* **2013**, *46*, 236−247. (j) Ritleng, V.; Sirlin, C.; Pfeffer, M. *Chem. Rev.* **2002**, *102*, 1731−1770. (k) Tang, R.-Y.; Li, G.; Yu, J.-Q. *Nature* **2014**, *507*, 215−220. (l) He, J.; Li, S.; Deng, Y.; Fu, H.; Laforteza, B. N.; Spangler, J. E.; Homs, A.; Yu, J.-Q. *Science* **2014**, *343*, 1216−1220.
(3) (a) Paull, D. H.; Abraham, C. J.; Scerba, M. T.; Alden-Danforth, E.; Lectka, T. *Acc. Chem. Res.* **2008**, *41*, 655−663. (b) Kanai, M.; Kato, N.; Ichikawa, E.; Shibasaki, M. *Synlett* **2005**, 1491−1508. (c) Allen, A. E.; MacMillan, D. W. C. *Chem. Sci.* **2012**, *3*, 633−658. (d) Piovesana, S.; Schietroma, D. M. S.; Bella, M. *Angew. Chem., Int. Ed.* **2011**, *50*, 6216−6232. (e) Ibrahem, I.; Córdova, A. *Angew. Chem., Int. Ed.* **2006**, *45*, 1952−1956. (f) Kumagai, N.; Shibasaki, M. *Angew. Chem., Int. Ed.* **2011**, *50*, 4760−4772.
(4) (a) Zhong, C.; Shi, X. *Eur. J. Org. Chem.* **2010**, 2999−3025. (b) Du, Z.; Shao, Z. *Chem. Soc. Rev.* **2013**, *42*, 1337−1378. (c) Shao, Z.; Zhang, H. *Chem. Soc. Rev.* **2009**, *38*, 2745−2755. (d) Vreese, R. B.; D'hooghe, M. *Beilstein J. Org. Chem.* **2012**, *8*, 398−402. (e) Parmar, D.; Sugiono, E.; Raja, S.; Rueping, M. *Chem. Rev.* **2014**, *114*, 9047−9153.
(5) (a) Nakao, Y.; Yada, A.; Hiyama, T. *J. Am. Chem. Soc.* **2010**, *132*, 10024−10026. (b) Sasai, H.; Suzuki, T.; Arai, S.; Arai, T.; Shibasaki, M. *J. Am. Chem. Soc.* **1992**, *114*, 4418−4420. (c) Sasai, H.; Arai, T.; Satow, Y.; Houk, K. N.; Shibasaki, M. *J. Am. Chem. Soc.* **1995**, *117*, 6194−6198. (d) Yamada, K.-i.; Harwood, S. J.; Gröger, H.; Shibasaki, M. *Angew. Chem., Int. Ed.* **1999**, *38*, 3504−3506. (e) Yamada, Y. M. A.; Yoshikawa, N.; Sasai, H.; Shibasaki, M. *Angew. Chem., Int. Ed.* **1997**, *36*, 1871−1873. (f) Arai, T.; Sasai, H.; Aoe, K.-i.; Okamura, K.; Date, T.; Shibasaki, M. *Angew. Chem., Int. Ed.* **1996**, *35*, 104−106. (g) Park, J.; Hong, S. *Chem. Soc. Rev.* **2012**, *41*, 6931−6943.
(6) (a) Zhao, X.; DiRocco, D. A.; Rovis, T. *J. Am. Chem. Soc.* **2011**, *133*, 12466−12469. (b) Denmark, S. E.; Burk, M. T. *Org. Lett.* **2012**, *14*, 256−259. (c) Serdyuk, O. V.; Zamfir, A.; Hampel, F.; Tsogoeva, S. B. *Adv. Synth. Catal.* **2012**, *354*, 3115−3121. (d) Uraguchi, D.; Ueki, Y.; Ooi, T. *Science* **2009**, *326*, 120−123. (e) Weil, T.; Kotke, M.; Kleiner, C. M.; Schreiner, P. R. *Org. Lett.* **2008**, *10*, 1513−1516.
(7) Patil, N. T.; Shinde, V. S.; Gajula, B. *Org. Biomol. Chem.* **2012**, *10*, 211−224.
(8) Tripathi, A.; Srivastava, U. C. *Annals of Neurosci.* **2008**, *15*, 106−111.
(9) (a) Knowles, R. R.; Jacobsen, E. N. *Proc. Natl. Acad. Sci. U. S. A.* **2010**, *107*, 20678−20685. (b) Warshel, A.; Sharma, P. K.; Kato, M.; Xiang, Y.; Liu, H.; Olsson, M. H. M. *Chem. Rev.* **2006**, *106*, 3210−3235.
(10) Raynal, M.; Ballester, P.; Vidal-Ferran, A.; van Leeuwen, P. W. N. M. *Chem. Soc. Rev.* **2014**, *43*, 1660−1733.
(11) (a) Janardanan, D.; Sunoj, R. B. *J. Org. Chem.* **2007**, *72*, 331−341. (b) Hammar, P.; Marcelli, T.; Hiemstra, H.; Himo, F. *Adv. Synth. Catal.* **2007**, *349*, 2537−2548. (c) Shinisha, C. B.; Sunoj, R. B. *Org. Biomol. Chem.* **2008**, *6*, 3921−3929. (d) Terada, M.; Soga, K.; Momiyama, N. *Angew. Chem., Int. Ed.* **2008**, *47*, 4122−4125. (e) Janardanan, D.; Sunoj, R. B. *J. Org. Chem.* **2008**, *73*, 8163−8174. (f) Patil, M. P.; Sunoj, R. B. *Chem.—Asian J.* **2009**, *4*, 714−724. (g) Shinisha, C. B.; Sunoj, R. B. *Org. Lett.* **2009**, *11*, 3242−3245. (h) Domingo, L. R.; Zaragoza, R. J.; Arno, M. *Org. Biomol. Chem.* **2010**, *8*, 4884−4891. (i) Patil, M. P.; Sharma, A. K.; Sunoj, R. B. *J. Org. Chem.* **2010**, *75*, 7310−7321. (j) Shinisha, C. B.; Sunoj, R. B. *Org. Lett.* **2010**, *12*, 2868−2871. (k) Cheong, P. H.-Y.; Legault, C. Y.; Um, J. M.; Çelebi-Ölçüm, N.; Houk, K. N. *Chem. Rev.* **2011**, *111*, 5042−5137. (l) Sharma, A. K.; Sunoj, R. B. *Chem. Commun.* **2011**, *47*, 5759−5761. (m) González, A. Z.; Benitez, D.; Tkatchouk, E.; Goddard, W. A.; Toste, F. D. *J. Am. Chem. Soc.* **2011**, *133*, 5500−5507. (n) Jindal, G.; Sunoj, R. B. *Org. Biomol. Chem.* **2012**, *10*, 7996−8006. (o) Zhu, J.-L.; Zhang, Y.; Liu, C.; Zheng, A.-M.; Wang, W. *J. Org. Chem.* **2012**, *77*, 9813−9825. (p) Jindal, G.; Sunoj, R. B. *Chem.—Eur. J.* **2012**, *18*, 7045−7049. (q) Zhang, W.; Zhu, Y.; Wei, D.; Li, Y.; Tang, M.-S. *J. Org. Chem.* **2012**, *77*, 10729−10737. (r) Reddi, Y.; Sunoj, R. B. *Org. Lett.* **2012**, *14*, 2810−2813. (s) Allen, S. E.; Mahatthananchai, J.; Bode, J. W.; Kozlowski, M. C. *J. Am. Chem. Soc.* **2012**, *134*, 12098−12103. (t) Sunoj, R. B.; Anand, M. *Phys. Chem. Chem. Phys.* **2012**, *14*, 12715−12736. (u) Anand, M.; Sunoj, R. B. *Organometallics* **2012**, *31*, 6466−6481. (v) Sharma, A. K.; Sunoj, R. B. *J. Org. Chem.* **2012**, *77*, 10516−10524. (w) Sengupta, A.; Sunoj, R. B. *J. Org. Chem.* **2012**, *77*, 10525−10536. (x) Yang, H.; Wong, M. W. *J. Am. Chem. Soc.* **2013**, *135*, 5808−5818. (y) Rajeev, R.; Sunoj, R. B. *J. Org. Chem.* **2013**, *78*, 7023−7029. (z) Coric, I.; Kim, J. H.; Vlaar, T.; Patil, M.; Thiel, W.; List, B. *Angew. Chem., Int. Ed.* **2013**, *52*, 3490−3493. (aa) Parija, A.; Sunoj, R. B. *Org. Lett.* **2013**, *15*, 4066−4069. (ab) Sanhueza, I. A.; Wagner, A. W.; Sanford, M. S.; Schoenebeck, F. *Chem. Sci.* **2013**, *4*, 2767−2775. (ac) Kuniyil, R.; Sunoj, R. B. *Org. Lett.* **2013**, *15*, 5040−5043. (ad) Jindal, G.; Sunoj, R. B. *Angew. Chem., Int. Ed.* **2014**, *53*, 4432−4436. (ae) Kótai, B.; Kardos, G.; Hamza, A.; Farkas, V.; Pápai, I.; Soós, T. *Chem.—Eur. J.* **2014**, *20*, 5631−5639. (af) Jindal, G.; Sunoj, R. B. *Org. Biomol. Chem.* **2014**, *12*, 2745−2753. (ag) Johnston, R. C.; Cohen, D. T.; Eichman, C. C.; Scheidt, K. A.; Cheong, P. H.-Y. *Chem. Sci.* **2014**, *5*, 1974−1982. (ah) Verma, P.; Verma, P.; Sunoj, R. B. *Org. Biomol. Chem.* **2014**, *12*, 2176−2179. (ai) Lalli, C.; Dumoulin, A.; Lebée, C.; Drouet, F.; Guérineau, V.; Touboul, D.; Gandon, V.; Zhu, J.; Masson, G. *Chem.—Eur. J.* **2014**, DOI: 10.1002/chem.201405286.
(12) (a) Jorgensen, W. L. *Science* **2004**, *303*, 1813−1818. (b) Bauschlicher, C. W., Jr.; Langhoff, S. R. *Science* **1991**, *254*, 394−398. (c) Clary, D. C. *Science* **2006**, *314*, 265−266. (d) McCammon, J. A. *Science* **1987**, *238*, 486−491. (e) Weinhold, F. *Nature* **2001**, *411*, 539−541.
(13) (a) Ramachary, D. B.; Reddy, Y. V. *Eur. J. Org. Chem.* **2012**, 865−887. (b) Kano, T.; Maruoka, K. *Chem. Sci.* **2013**, *4*, 907−915. (c) Beeson, T. D.; Mastracchio, A.; Hong, J.; Ashton, K.; MacMillan, D. W. C. *Science* **2007**, *316*, 582−585. (d) Erkkilä, A.; Majander, I.; Pihko, P. M. *Chem. Rev.* **2007**, *107*, 5416−5470. (e) Doyagüez, E. G.; Calderón, F.; Sánchez, F.; Fernádez-Mayoralas, A. *J. Org. Chem.* **2007**, *72*, 9353−9356. (f) Jiang, Z.; Ye, W.; Yang, Y.; Tan, C.-H. *Adv. Synth. Catal.* **2008**, *350*, 2345−2351. (g) Kumaragurubaran, N.; Juhl, K.; Zhuang, W.; Bøgevig, A.; Jørgensen, K. A. *J. Am. Chem. Soc.* **2002**, *124*, 6254−6255. (h) Zhong, G. *Angew. Chem., Int. Ed.* **2003**, *42*, 4247−4250. (i) Enders, D.; Seki, A. *Synlett* **2002**, 26−28.
(14) (a) Marcelli, T.; Hiemstra, H. *Synthesis* **2010**, *8*, 1229−1279. (b) Marcelli, T. *WIREs Comp. Mol. Sci.* **2011**, *1*, 142−152. (c) Dijkstra, G. D. H.; Kellogg, R. M.; Wynberg, H. *J. Org. Chem.* **1990**, *55*, 6121−6131. (d) Schurch, M.; Schwalm, O.; Mallat, T.; Weber, J.; Baiker, A. *J. Catal.* **1997**, *169*, 275−286. (e) Burgi, T.; Vargas, A.; Baiker, A. *J. Chem. Soc., Perkin Trans. 2* **2002**, 1596−1601. (f) Denmark, S. E.; Beutner, G. L. *Angew. Chem., Int. Ed.* **2008**, *47*, 1560−1638. (g) Hiemstra, H.; Wynberg, H. *J. Am. Chem. Soc.* **1981**, *103*, 417−430. (h) Cucinotta, C. S.; Kosa, M.; Melchiorre, P.; Cavalli, A.; Gervasio, F. L. *Chem.—Eur. J.* **2009**, *15*, 7913−7921. (I) Duan, J.; Li, P. *Catal. Sci. Technol.* **2014**, *4*, 311−320. (j) Zheng, S.; Schienebeck, C. M.; Zhang, W.; Wang, H.-Y.; Tang, W. *Asian J. Org. Chem.* **2014**, *3*, 366−376. (k) Zhao, Y.-L.; Wang, Y.; Cao, J.; Liang, Y.-M.; Xu, P.-F. *Org. Lett.* **2014**, *16*, 2438−2441. (l) Noole, A.; Ilmarinen, K.; Järving, I.; Lopp, M.; Kanger, T. *J. Org. Chem.* **2013**, *78*, 8117−8122. (m) Saidalimu, I.; Fang, X.; He, X.-P.; Liang, J.; Yang, X.; Wu, F. *Angew. Chem., Int. Ed.* **2013**, *52*, 5566−5570.

(n) Asano, K.; Matsubara, S. *J. Am. Chem. Soc.* **2011**, *133*, 16711−16713. (o) Russo, A.; Galdi, G.; Croce, G.; Lattanzi, A. *Chem.—Eur. J.* **2012**, *18*, 6152−6157. (p) Song, J.; Wang, Y.; Deng, L. *J. Am. Chem. Soc.* **2006**, *128*, 6048−6049. (q) Hynes, P. S.; Stranges, D.; Stupple, P. A.; Guarna, A.; Dixon, D. J. *Org. Lett.* **2007**, *9*, 2107−2110.

(15) (a) Enders, D.; Balensiefer, T. *Acc. Chem. Res.* **2004**, *37*, 534−541. (b) Enders, D.; Niemeier, O.; Henseler, A. *Chem. Rev.* **2007**, *107*, 5606−5655. (c) Nair, V.; Vellalath, S.; Babu, B. P. *Chem. Soc. Rev.* **2008**, *37*, 2691−2698. (d) Phillips, E. M.; Chan, A.; Scheidt, K. A. *Aldrichimica Acta* **2009**, *42*, 55−66. (e) Vora, H. M.; Rovis, T. *Aldrichimica Acta* **2011**, *44*, 3−11. (f) Izquierdo, J.; Hutson, G. E.; Cohen, D. T.; Scheidt, K. A. *Angew. Chem., Int. Ed.* **2012**, *51*, 11686−11698. (g) Zhu, Z.-Q.; Zheng, X.-L.; Jiang, N. F.; Wan, X.; Xiao, J.-C. *Chem. Commun.* **2011**, *47*, 8670−8672. (h) Rong, Z.-Q.; Jia, M.-Q.; You, S.-L. *Org. Lett.* **2011**, *13*, 4080−4083. (i) Piel, I.; Steinmetz, M.; Hirano, K.; Frohlich, R.; Grimme, S.; Glorious, F. *Angew. Chem., Int. Ed.* **2011**, *50*, 4983−4987. (j) Ozboya, K. E.; Rovis, T. *Chem. Sci.* **2011**, *2*, 1835−1838. (k) Wanner, B.; Mahatthananchai, J.; Bode, J. W. *Org. Lett.* **2011**, *13*, 5378−5381. (l) Raup, D. E. A.; Cardinal-David, B.; Holte, D.; Scheidt, K. A. *Nat. Chem.* **2010**, *2*, 766−771.

(16) (a) Akiyama, T. *Chem. Rev.* **2007**, *107*, 5744−5758. (b) Zamfir, A.; Schenker, S.; Freund, M.; Tsogoeva, S. B. *Org. Biomol. Chem.* **2010**, *8*, 5262−5276. (c) Rueping, M.; Kuenkel, A.; Atodiresei, I. *Chem. Soc. Rev.* **2011**, *40*, 4539−4549. (d) Terada, M. *Chem. Commun.* **2008**, 4097−4112. (e) Zhang, Z.; Schreiner, P. R. *Chem. Soc. Rev.* **2009**, *38*, 1187−1198. (f) Zhang, Z.; Jain, P.; Antilla, J. C. *Angew. Chem., Int. Ed.* **2011**, *50*, 10961−10964. (g) Wang, P.-S.; Zhou, X.-L.; Gong, L.-Z. *Org. Lett.* **2014**, *16*, 976−979. (h) Seayad, J.; Seayad, A. M.; List, B. *J. Am. Chem. Soc.* **2006**, *128*, 1086−1087. (i) Terada, M.; Tanaka, H.; Sorimachi, K. *J. Am. Chem. Soc.* **2009**, *131*, 3430−3431. (j) Rueping, M.; Sugiono, E.; Azap, C. *Angew. Chem., Int. Ed.* **2006**, *45*, 2617−2619. (k) Mori, K.; Wakazawa, M.; Akiyama, T. *Chem. Sci.* **2014**, *5*, 1799−1803. (l) Bandini, M.; Bottoni, A.; Chiarucci, M.; Cera, G.; Miscione, G. P. *J. Am. Chem. Soc.* **2012**, *134*, 20690−20700.

(17) (a) Akiyama, T.; Itoh, J.; Yokota, K.; Fuchibe, K. *Angew. Chem., Int. Ed.* **2004**, *43*, 1566−1568. (b) Uraguchi, D.; Terada, M. *J. Am. Chem. Soc.* **2004**, *126*, 5356−5357.

(18) (a) Akiyama, T.; Itoh, J.; Fuchibe, K. *Adv. Synth. Catal.* **2006**, *348*, 999−1010. (b) Taylor, M. S.; Jacobsen, E. N. *Angew. Chem., Int. Ed.* **2006**, *45*, 1520−1543.

(19) (a) Simón, L.; Goodman, J. M. *J. Am. Chem. Soc.* **2008**, *130*, 8741−8747. (b) Grayson, M. N.; Goodman, J. M. *J. Am. Chem. Soc.* **2013**, *135*, 6142−6148. (c) Shibata, Y.; Yamanaka, M. *J. Org. Chem.* **2013**, *78*, 3731−3736. (d) Wang, H.; Jain, P.; Antilla, J. C.; Houk, K. N. *J. Org. Chem.* **2013**, *78*, 1208−1215. (e) Yamanaka, M.; Hirata, T. *J. Org. Chem.* **2009**, *74*, 3266−3271.

(20) (a) Lacour, J.; Moraleda, D. *Chem. Commun.* **2009**, 7073−7089. (b) Brak, K.; Jacobsen, E. N. *Angew. Chem., Int. Ed.* **2013**, *52*, 534−561.

(21) (a) Lacour, J.; Linder, D. *Science* **2007**, *317*, 462−463. (b) Ohmatsu, K.; Ito, M.; Kunieda, T.; Ooi, T. *Nat. Chem.* **2012**, *4*, 473−477.

(22) (a) Phipps, R. J.; Hamilton, G. L.; Toste, F. D. *Nat. Chem.* **2012**, *4*, 603−614. and the references therein (b) Mahlau, M.; List, B. *Angew. Chem., Int. Ed.* **2013**, *52*, 518−533.

(23) Mayer, S.; List, B. *Angew. Chem., Int. Ed.* **2006**, *45*, 4193−4195.

(24) Parra, A.; Reboredo, S.; Castroa, A. M. M.; Alemán, J. *Org. Biomol. Chem.* **2012**, *10*, 5001−5020.

(25) Rueping, M.; Antonchick, A. P.; Brinkmann, C. *Angew. Chem., Int. Ed.* **2007**, *46*, 6903−6906.

(26) Hamilton, G. L.; Kang, J. E.; Mba, M.; Toste, F. D. *Science* **2007**, *317*, 496−499.

(27) Rueping, M.; Koenigs, R. M.; Atodiresei, I. *Chem.—Eur. J.* **2010**, *16*, 9350−9365.

(28) Barbazanges, M.; Augé, M.; Moussa, J.; Amouri, H.; Aubert, C.; Desmarets, C.; Fensterbank, L.; Gandon, V.; Malacria, M.; Ollivier, C. *Chem.—Eur. J.* **2011**, *17*, 13789−13794.

(29) Arthuis, M.; Beaud, R.; Gandon, V.; Roulland, E. *Angew. Chem., Int. Ed.* **2012**, *51*, 10510−10514.

(30) Tang, W.; Johnston, S.; Iggo, J. A.; Berry, N. G.; Phelan, M.; Lian, L.; Bacsa, J.; Xiao, J. *Angew. Chem., Int. Ed.* **2013**, *52*, 1668−1672.

(31) (a) Jiang, G.; List, B. *Angew. Chem., Int. Ed.* **2011**, *50*, 9471−9474. (b) Mukherjee, S.; List, B. *J. Am. Chem. Soc.* **2007**, *129*, 11336−11337.

(32) Jindal, G.; Sunoj, R. B. *J. Org. Chem.* **2014**, *76*, 7600−7606.

(33) Fleischmann, M.; Drettwan, D.; Sugiono, E.; Rueping, M.; Gschwind, R. M. *Angew. Chem., Int. Ed.* **2011**, *50*, 6364−6369.

(34) (a) Meot-Ner (Mautner), M. *Chem. Rev.* **2012**, *112*, PR22−PR103. (b) Butts, C. P.; Filali, E.; Lloyd-Jones, G. C.; Norrby, P.-O.; Sale, D. A.; Schramm, Y. *J. Am. Chem. Soc.* **2009**, *131*, 9945−9957.

(35) (a) Kumara Swamy, K. C.; Kumaraswamy, S.; Kommana, P. *J. Am. Chem. Soc.* **2001**, *123*, 12642−12649. (b) Raymo, F. M.; Bartberger, M. D.; Houk, K. N.; Stoddart, J. F. *J. Am. Chem. Soc.* **2001**, *123*, 9264−9267.

(36) Jindal, G.; Sunoj, R. B. *J. Am. Chem. Soc.* **2014**, *136*, 15998−16008.

(37) Chai, Z.; Rainey, T. J. *J. Am. Chem. Soc.* **2012**, *134*, 3615−3618.

(38) (a) Wang, B.; Tu, Y. Q. *Acc. Chem. Res.* **2011**, *44*, 1207−1222. (b) Franz, A. K.; Hanhan, N. V.; Ball-Jones, N. *ACS Catal.* **2013**, *3*, 540−553. (c) Zhang, Q.-W.; Fan, C.-A.; Zhang, H.-J.; Tu, Y.-Q.; Zhao, Y.-M.; Gu, P.; Chen, Z.-M. *Angew. Chem., Int. Ed.* **2009**, *48*, 8572−8574. (d) D'yakonov, V. A.; Trapeznikova, O. A.; de Meijere, A.; Dzhemilev, U. M. *Chem. Rev.* **2014**, *114*, 5775−5814.

(39) Engelin, C. J.; Jensen, T.; Rodríguez-Rodríguez, S.; Fristrup, P. *ACS Catal.* **2013**, *3*, 294−302.

(40) (a) Davies, H. M. L. *Angew. Chem., Int. Ed.* **2006**, *45*, 6422−6425. (b) Terada, M.; Toda, Y. *Angew. Chem., Int. Ed.* **2012**, *51*, 2093−2097. (c) Jiang, J.; Xu, H.-D.; Xi, J.-B.; Ren, B.-Y.; Lv, F.-P.; Guo, X.; Jiang, L.-Q.; Zhang, Z.-Y.; Hu, W.-H. *J. Am. Chem. Soc.* **2011**, *133*, 8428−8431. (d) Qiu, H.; Li, M.; Jiang, L.-Q.; Lv, F.-P.; Zan, L.; Zhai, C.-W.; Doyle, M. P.; Hu, W.-H. *Nat. Chem.* **2012**, *4*, 733−738. (e) Hu, W.; Xu, X.; Zhou, J.; Liu, W.-J.; Huang, H.; Hu, J.; Yang, L.; Gong, L.-Z. *J. Am. Chem. Soc.* **2008**, *130*, 7782−7783.

(41) (a) Gulevich, A. V.; Gevorgyan, V. *Angew. Chem., Int. Ed.* **2013**, *52*, 1371−1373. (b) Doyle, M. P.; Duffy, R.; Ratnikov, M.; Zhou, L. *Chem. Rev.* **2010**, *110*, 704−724. (c) Wang, X.; Abrahams, Q. M.; Zavalij, P. Y.; Doyle, M. P. *Angew. Chem., Int. Ed.* **2012**, *51*, 5907−5910. (d) Selander, N.; Worrell, B. T.; Fokin, V. V. *Angew. Chem., Int. Ed.* **2012**, *51*, 13054−13057. (e) Davies, H. M. L.; Manning, J. R. *Nature* **2008**, *451*, 417−424. (f) Kornecki, K. P.; Briones, J. F.; Boyarskikh, V.; Fullilove, F.; Autschbach, J.; Schrote, K. E.; Lancaster, K. M.; Davies, H. M. L.; Berry, J. F. *Science* **2013**, *342*, 351−354. (g) Jat, J. L.; Paudyal, M. P.; Gao, H.; Xu, Q.-L.; Yousufuddin, M.; Devarajan, D.; Ess, D. H.; Kürti, L.; Falck, J. R. *Science* **2014**, *343*, 61−65. (h) Li, Z.; Boyarskikh, V.; Hansen, J. H.; Autschbach, J.; Musaev, D. G.; Davies, H. M. L. *J. Am. Chem. Soc.* **2012**, *134*, 15497−15504.

(42) (a) Ye, T.; McKervey, M. A. *Chem. Rev.* **1994**, *94*, 1091−1160. (b) Zhang, Z.-H.; Wang, J.-B. *Tetrahedron* **2008**, *64*, 6577−6605. (c) Moody, C. J.; Ferris, L.; Haigh, D.; Swann, E. *Chem. Commun.* **1997**, 2391−2392. (d) Bolm, C.; Kasyan, A.; Drauz, K.; Gunther, K.; Raabe, G. *Angew. Chem., Int. Ed.* **2000**, *39*, 2288−2290. (e) Davies, J. R.; Kane, P. D.; Moody, C. J. *J. Org. Chem.* **2005**, *70*, 7305−7316. (f) Shi, B.; Blake, A. J.; Lewis, W.; Campbell, I. B.; Judkins, B. D.; Moody, C. J. *J. Org. Chem.* **2010**, *75*, 152−161.

(43) Chuprakov, S.; Malik, J. A.; Zibinsky, M.; Fokin, V. V. *J. Am. Chem. Soc.* **2011**, *133*, 10352−10355.

(44) Xu, B.; Zhu, S.-F.; Xie, X.-L.; Shen, J.-J.; Zhou, Q.-L. *Angew. Chem., Int. Ed.* **2011**, *50*, 11483−11486.

(45) Xu, B.; Zhu, S.-F.; Zhang, Z.-C.; Yu, Z.-X.; Maa, Y.; Zhou, Q.-L. *Chem. Sci.* **2014**, *5*, 1442−1448.

(46) Wang, X.-C.; Song, X.-S.; Guo, L.-P.; Qu, D.; Xie, Z.-Z.; Verpoort, F.; Cao, J. *Organometallics* **2014**, *33*, 4042−4050.
(47) Kisan, H. K.; Sunoj, R. B. *Chem. Commun.* **2014**, *50*, 14639−14642.
(48) (a) Katayev, D.; Banarjee, D.; Jia, Y.-X.; Besnard, C.; Sharma, A. K.; Sunoj, R. B.; Kundig, P. E. *Chem.—Eur. J.* **2013**, *19*, 11916−11927. (b) John, A.; Ghosh, P. *Dalton Trans.* **2010**, *39*, 7183−7206. (c) Glorius, F.; Altenhoff, G.; Goddard, R.; Lehmann, C. *Chem. Commun.* **2002**, 2704−2705. (d) Luan, X.; Mariz, R.; Robert, C.; Gatti, M.; Blumentritt, S.; Linden, A.; Dorta, R. *Org. Lett.* **2008**, *10*, 5569−5572. (e) Wu, L.; Falivene, L.; Drinkel, E.; Grant, S.; Linden, A.; Cavallo, L.; Dorta, R. *Angew. Chem., Int. Ed.* **2012**, *51*, 2870−2873. (f) Spallek, M. J.; Riedel, D.; Rominger, F.; Hashmi, A. S. K.; Trapp, O. *Organometallics* **2012**, *31*, 1127−1132.
(49) (a) Lebeuf, R.; Hirano, K.; Glorius, F. *Org. Lett.* **2008**, *10*, 4243−4246. (b) Burgess, K.; Perry, M. C. *Tetrahedron: Asymmetry* **2003**, *14*, 951−961. (c) Wurz, S.; Glorious, F. *Acc. Chem. Res.* **2008**, *41*, 1523−1533. (d) Nolan, P. *Acc. Chem. Res.* **2011**, *44*, 91−100.
(50) Cohen, D. T.; Scheidt, K. A. *Chem. Sci.* **2012**, *3*, 53−57.
(51) Domingo, L. R.; Zaragozá, R. J.; Arnó, M. *Org. Biomol. Chem.* **2011**, *9*, 6616−6622.
(52) Deng, Y.; Kumar, S.; Wang, H. *Chem. Commun.* **2014**, *50*, 4272−4284.
(53) Stegbauer, L.; Sladojevich, F.; Dixon, D. J. *Chem. Sci.* **2012**, *3*, 942−958.
(54) Ibrahem, I.; Santoro, S.; Himo, F.; Córdova, A. *Adv. Synth. Catal.* **2011**, *353*, 245−252.
(55) Patil, N. T.; Nijamudheen, A.; Datta, A. *J. Org. Chem.* **2012**, *77*, 6179−6185.
(56) Sladojevich, F.; Fuentes de Arriba, A. L.; Ortín, I.; Yang, T.; Ferrali, A.; Paton, R. S.; Dixon, D. J. *Chem.—Eur. J.* **2013**, *19*, 14286−14295.
(57) Xu, H.; Zeund, S. J.; Woll, M. G.; Tao, Y.; Jacobsen, E. N. *Science* **2010**, *327*, 986−990.
(58) Zhang, Z.; Lippert, K. M.; Hausmann, H.; Kotke, M.; Schreiner, P. R. *J. Org. Chem.* **2011**, *76*, 9764−9776.
(59) (a) Maeda, S.; Komagawa, S.; Uchiyama, M.; Morokuma, K. *Angew. Chem., Int. Ed.* **2011**, *50*, 644−649. (b) Rooks, B. J.; Haas, M. R.; Sepulveda, D.; Lu, T.; Wheeler, S. E. *ACS Catal.* **2014**, DOI: 10.1021/cs5012553.